

Measure-theoretical properties of the unstable foliation of two-dimensional differentiable area-preserving systems

A. Adrover and M. Giona

Dipartimento di Ingegneria Chimica, Università di Roma "La Sapienza," via Eudossiana 18, 00184 Roma, Italy

(Received 23 November 1998)

This article analyzes in detail the statistical and measure-theoretical properties of the nonuniform stationary measure, referred to as the w -invariant measure, associated with the spatial length distribution of the integral manifolds of the unstable invariant foliation in two-dimensional differentiable area-preserving systems. The analysis is developed starting from a sequence of analytical approximations for the associated density. These approximations are related to the properties of the Jacobian matrix of the n th iteration of a Poincaré map. The w -invariant measure plays a fundamental role in the study of transport phenomena in laminar-chaotic fluid-mixing systems, for which it furnishes the asymptotic invariant distribution of intermaterial contact length between two fluids. The w -invariant measure turns out to be singular and exhibits multifractal features. Its associated density displays local self-similarity in an ε neighborhood of hyperbolic periodic points. The cancellation exponent of the signed measure associated with the w measure by attaching at each point the direction of the field of the asymptotic unstable eigenvectors is also analyzed. The only case for which the w -invariant measure is absolutely continuous is given by the conjugation of hyperbolic toral automorphisms with a linear automorphism. The connections with the statistical properties, and in particular with the stretching dynamics, are addressed in detail. [S1063-651X(99)15405-9]

PACS number(s): 05.45.-a, 84.40.Ik, 47.53.+n, 83.50.Ws

I. INTRODUCTION

In many physical problems involving chaotic Hamiltonian systems and symplectic maps, the central issue is given by the evolution of vectors and line elements and of curve arcs advected by the dynamics. Examples include the fast dynamo problems in magnetohydrodynamics (for high values of the magnetic Reynolds number) [1,2], where attention is focused on the properties of the magnetic field or fluid dynamic phenomena involving incompressible flows [3,4], where interfacial phenomena are controlled by the statistical properties associated with the evolution of curves [in two-dimensional (2D) systems] or of surfaces (in 3D systems), since they form interfaces between different fluid elements [5].

The evolution of interfaces advected by chaotic flows controls many dynamic phenomena in fluid systems and its understanding is the starting point for a theory of transport and reaction in laminar chaotic flows [6,7]. If the diffusive mass transfer is small compared to the convective contribution (i.e., if the Péclet number is sufficiently high), the effects of diffusion may be overlooked at short or intermediate time scales. Under these conditions, the kinematics of a passive tracer particle is described by an ordinary differential equation [8,9]

$$\frac{d\mathbf{x}(t)}{dt} = \mathbf{v}(\mathbf{x}(t), t), \quad (1.1)$$

where \mathbf{v} is a time-dependent velocity field and $\mathbf{x} = (x, y)^t$ the position vector of the advected particle. This situation customarily occurs for highly viscous fluids and polymeric solutions, which constitute the natural realm of laminar chaotic flows.

As observed by Aref in 1984 [8], 2D incompressible fluid flows in laminar conditions (i.e., if the inertial contribution is negligible with respect to the viscous) are perfectly equivalent to Hamiltonian systems through identification of the stream function with the Hamiltonian and the physical space with the phase space of Hamiltonian dynamics. This is because, under the conditions stated above, the velocity field \mathbf{v} in Eq. (1.1) can be related to the partial derivatives of the stream function ψ as $\mathbf{v} = (\partial\psi/\partial y, -\partial\psi/\partial x)^t$. This equivalence makes it possible to extrapolate the simulation and experimental results obtained by considering laminar fluid motion to Hamiltonian systems and vice versa.

It has been observed both numerically and experimentally that area-preserving dynamics (such as incompressible fluid flows) display invariant patterns in the evolution of line elements advected by the velocity field \mathbf{v} under the condition that the dynamical system Eq. (1.1) is chaotic [10,11] (see Sec. II for a formal definition of chaos). These invariant properties have been attributed to the dominant role of the unstable manifolds of hyperbolic periodic points which are dense within a chaotic region [12]. The geometrical explanation of this phenomenon lies in the fact that the restriction of a Poincaré section of a time-periodic 2D differentiable area-preserving flow within a chaotic region defines upon it a hyperbolic map (see Sec. III for a thorough analysis of this point), thus inheriting the global geometrical properties characterizing these systems. In particular, within the tangent space of each point \mathbf{x} of an invariant chaotic region, an unstable direction $\mathbf{e}^u(\mathbf{x})$ may be defined which is tangent to any material line passing through \mathbf{x} that has evolved for a sufficiently long time. The hyperbolic nature of a chaotic differentiable area-preserving dynamics determines not only the geometry and topology of mixing (since it defines the asymptotic unstable direction $\mathbf{e}^u(\mathbf{x})$ attained by tangent vectors to fluid interfaces), but enables us to frame in a quanti-

tative way the measure-theoretical and statistical properties in the evolution of material interfaces as an intrinsic property of the spatial length distribution of a generic integral manifold belonging to the unstable foliation.

In a previous article [13], it was shown that hyperbolic area-preserving maps on the torus conjugate to a linear one are characterized by a nonuniform measure associated with the length distribution of the contact interface between fluid elements. This measure is intrinsically different from the uniform ergodic measure and may be viewed as the invariant measure associated with the dynamical systems generated by the unstable vector field $\mathbf{e}^u(\mathbf{x})$. This new measure has been referred to as the w -invariant measure. The extension of this result to generic area-preserving 2D differentiable dynamics is given in Ref. [14].

This article analyzes in greater detail the structure and properties of the w -invariant measure for generic area-preserving chaotic differentiable dynamical systems defined by Eq. (1.1), and provides several ways to compute it directly from the differential of the n th iterative of the Poincaré map of the flow. The statistical and singular properties of this measure are addressed in detail since, for a generic area-preserving map, the w -invariant measure possesses multifractal scaling properties and a sign-singular measure may be associated with it. To complete the analysis, the connection between stretching dynamics and w -invariant measure is thoroughly examined since it provides striking evidence of the close connections between global geometric invariant features and statistical properties.

This article is organized as follows. Section II introduces the basic definitions and the model systems considered. Section III develops a succinct but self-contained analysis of the hyperbolicity and orientational properties of differentiable area-preserving dynamics. Section IV addresses the geometric structure of the unstable foliation as well as its relation with the evolution of material lines and defines the w -invariant measure. Section V develops closed-form expressions for a sequence of approximants of the w -invariant density, by making use of the invariant orientational properties of chaotic differentiable area-preserving dynamics. Convergence properties are also addressed. Section VI analyzes the singularity structure of the w -invariant measure through multifractal analysis and through the cancellation exponent of the associated signed measure defined starting from the field of unstable eigenvectors. Section VII develops the connection between the w -invariant density and stretching dynamics, thus providing an alternative expression for a sequence of approximants of the w density based on the multiplicative stretching dynamics.

II. MODEL SYSTEMS AND BASIC DEFINITIONS

Throughout this article, 2D time-periodic area-preserving differentiable dynamical systems of the form given by Eq. (1.1) are considered. The velocity field \mathbf{v} therefore satisfies the condition $\mathbf{v}(\mathbf{x}, t + T) = \mathbf{v}(\mathbf{x}, t)$, where T is the period of the perturbation. Φ is used to indicate the Poincaré map associated with Eq. (1.1), obtained by sampling the trajectories modulo the period T . In this way, the dynamics is described by means of an autonomous dynamical system.

$$\mathbf{x}_{n+1} = \Phi(\mathbf{x}_n), \quad (2.1)$$

where $\mathbf{x}_n = \mathbf{x}(nT)$, defined on a two-dimensional manifold M . Attention is restricted to differentiable dynamics. We therefore assume that Φ is at least a C^2 diffeomorphism, i.e., *fortiori* that both Φ and its inverse Φ^{-1} are differentiable and their Jacobian matrices continuous.

We use the term $\Phi^*(\mathbf{x}) = \partial\Phi(\mathbf{y})/\partial\mathbf{y}|_{\mathbf{y}=\mathbf{x}}$ to indicate the differential of Φ at \mathbf{x} , i.e., its Jacobian matrix. $\Phi^*(\mathbf{x})$ is a mapping of the tangent space $TM_{\mathbf{x}}$ at \mathbf{x} onto the tangent space $TM_{\Phi^*(\mathbf{x})}$ at the image point. The differential $\Phi^*(\mathbf{x})$ is the basic mapping in order to analyze the first-order properties of the Poincaré map Φ , and in particular the evolution of vectors tangent to curves (representing the boundary of a fluid-phase-space element) advected by the velocity field \mathbf{v} . The condition of area preservation means that the determinant of the differential is in absolute value equal to 1 for all $\mathbf{x} \in M$. In the case of the dynamical system considered, the more restrictive condition $\det(\Phi^*(\mathbf{x})) = 1$ holds, thus implying that the differentials $\Phi^*(\mathbf{x})$ for $\mathbf{x} \in M$ belong to the group of unimodular matrices $SL(2, \mathbb{R})$. By definition, the differential $\Phi^{n*}(\mathbf{x})$ of the n th iterative of Φ is given by

$$\begin{aligned} \Phi^{n*}(\mathbf{x}) &= \Phi^*(\Phi^{n-1}(\mathbf{x})) \cdot \Phi^*(\Phi(\mathbf{x})) \cdot \Phi^*(\mathbf{x}) \\ &= \prod_{j=0}^{n-1} \Phi^*(\Phi^j(\mathbf{x})). \end{aligned}$$

The definition of stretching can be directly referred to the action of the differential. Given a vector $\mathbf{v} \in TM_{\mathbf{x}}$, the stretching after n steps at \mathbf{x} can be defined as $\lambda^{(n)}(\mathbf{x}, \mathbf{v}/\|\mathbf{v}\|) = \|\Phi^{n*}(\mathbf{x})\mathbf{v}\|/\|\mathbf{v}\|$. This definition for the stretching at a point depends not only on \mathbf{x} but also on the orientation of the initial vector, i.e., on $\mathbf{v}/\|\mathbf{v}\|$.

We assume a fairly general definition of chaos for area-preserving mappings. A map Φ is said to be chaotic within an invariant submanifold $C \subseteq M$ if, for each $\mathbf{x} \in C$ and for any vector $\mathbf{v} \in TC_{\mathbf{x}}$, the sequence of vectors $\Phi^{n*}(\mathbf{x})\mathbf{v}$ is unbounded in norm, either forward ($n \rightarrow \infty$) or backward ($n \rightarrow -\infty$) in time [15], i.e.,

$$\sup_{-\infty < n < \infty} \|\Phi^{n*}(\mathbf{x})\mathbf{v}\| = \infty. \quad (2.2)$$

This definition is related to the sensitive dependence with respect to the initial conditions typical of chaotic dynamical systems, since the distance between the evolution of nearby points $\|\Phi^n(\mathbf{x} + \varepsilon) - \Phi^n(\mathbf{x})\|$ for small ε can be expanded to the first order to give $\|\Phi^{n*}(\mathbf{x})\varepsilon\| \sim \exp(n\lambda)\|\varepsilon\|$ with $\lambda > 0$.

Throughout this article we consider three representative models of area-preserving differentiable dynamics in two dimensions: the standard map, the Duffing oscillator, and a family of toral diffeomorphisms conjugated to a linear hyperbolic one. The standard map, introduced by Chirikov [16] is defined on the two-dimensional torus and is given by

$$\begin{cases} x_{n+1} = x_n - (\kappa/2\pi)\sin(2\pi y_n) \pmod{1} \\ y_{n+1} = y_n + x_{n+1} \pmod{1}. \end{cases} \quad (2.3)$$

For $\kappa > \kappa^* \approx 0.97$ (value of the parameter κ corresponding to the breakup of the last KAM torus [17]) there exists one region (at least) in the phase space within which the map is chaotic.

The Duffing oscillator is another typical prototype of Hamiltonian chaos [18]. The equations of motion are

$$\begin{aligned} \dot{x} &= y, \\ \dot{y} &= x - x^3 + \gamma \cos(\omega t), \end{aligned} \quad (2.4)$$

where $\dot{x} = dx/dt$ and corresponds to a nonlinear oscillator with a 2-4 potential in the presence of a sinusoidal perturbation. An analytical expression for the Poincaré map Φ is not available for the Duffing oscillator and it should therefore be computed numerically. The variables x , y and time (t or n) entering into Eqs. (2.3) and (2.4) are considered to be made dimensionless upon a suitable variable rescaling.

We also consider another prototype of chaotic dynamics on the two-dimensional torus \mathcal{T}^2 . Given the linear toral automorphism $\mathcal{B}(\mathbf{x}) = \mathbf{B}\mathbf{x} \bmod 1$, expressed by the integer-value matrix \mathbf{B} [19]

$$\mathbf{B} = \begin{pmatrix} 1 & 1 \\ 1 & 2 \end{pmatrix}, \quad (2.5)$$

and a family area-preserving diffeomorphism \mathcal{H} of the torus, a family of dynamical systems Φ can be constructed, topologically conjugate with \mathcal{B} ,

$$\Phi = \mathcal{H}^{-1} \circ \mathcal{B} \circ \mathcal{H}, \quad (2.6)$$

where \circ indicates composition. Since \mathcal{B} is globally chaotic within \mathcal{T}^2 (and is indeed a classical example of a uniformly hyperbolic system on a two-dimensional manifold [19,20]—also see Sec. III), Φ also possesses the same properties. Topological conjugacy implies that the trajectories of \mathcal{B} are mapped onto the trajectories of Φ so that

$$\Phi^n = \mathcal{H}^{-1} \circ \mathcal{B}^n \circ \mathcal{H}. \quad (2.7)$$

This class of systems has been extensively investigated in Refs. [13, 21] and is particularly suitable for analytical investigation since closed-form expressions for its trajectories can be easily obtained due to the linearity of \mathcal{B} . As a candidate for \mathcal{H} , the standard map defined by Eq. (2.3) may be chosen.

The family of toral diffeomorphisms Eq. (2.6) is particularly interesting for the purposes of this article for two main reasons: (1) a closed-form expression for the w measure is available [13] and (2) their w measures possess basic differences with respect to the corresponding measures defined for maps associated with physically realizable Hamiltonian systems such as the Duffing oscillator and the standard map (see Secs. VI and VII).

III. HYPERBOLICITY AND ORIENTATIONAL PROPERTIES OF DIFFERENTIABLE DYNAMICS

Hyperbolicity is the key concept applied to infer the global geometric features of differentiable dynamics [19,20,22]. Essentially, a diffeomorphic map Φ is hyperbolic (or Anosov) on an invariant submanifold \mathcal{C} if it induces a splitting of the tangent space $T\mathcal{C}_{\mathbf{x}}$ at any \mathbf{x} belonging to \mathcal{C} into two vector subspaces $\mathcal{E}_{\mathbf{x}}^u$ (the unstable or dilating subspace) and $\mathcal{E}_{\mathbf{x}}^s$ (the stable or contracting subspace):

$$T\mathcal{C}_{\mathbf{x}} = \mathcal{E}_{\mathbf{x}}^u \oplus \mathcal{E}_{\mathbf{x}}^s, \quad (3.1)$$

where \oplus indicates direct sum of vector subspaces. The unstable and (stable) vector sub-bundles $\{\mathcal{E}_{\mathbf{x}}^u\}_{\mathbf{x} \in \mathcal{C}}$, ($\{\mathcal{E}_{\mathbf{x}}^s\}_{\mathbf{x} \in \mathcal{C}}$) are invariant under the differential, i.e.,

$$\Phi^*(\mathbf{x})|_{\mathcal{E}_{\mathbf{x}}^u} = \mathcal{E}_{\Phi(\mathbf{x})}^u, \quad \Phi^*(\mathbf{x})|_{\mathcal{E}_{\mathbf{x}}^s} = \mathcal{E}_{\Phi(\mathbf{x})}^s, \quad (3.2)$$

and possess the dynamic properties of expanding (contracting) vectors. In particular, for uniformly hyperbolic systems (uniformly Anosov), the expanding properties of $\mathcal{E}_{\mathbf{x}}^u$ and the contracting properties of $\mathcal{E}_{\mathbf{x}}^s$ are uniform in \mathcal{C} , which implies that there exist constants $a, b, c, d > 0$ and $\lambda > 1$ such that if $\mathbf{v}_u \in \mathcal{E}_{\mathbf{x}}^u$ and $\mathbf{v}_s \in \mathcal{E}_{\mathbf{x}}^s$ then

$$\|\Phi^{n*}(\mathbf{x})\mathbf{v}_u\| \geq a\lambda^n \|\mathbf{v}_u\|, \quad \|(\Phi^{-n})^*(\mathbf{x})\mathbf{v}_u\| \leq b\lambda^{-n} \|\mathbf{v}_u\|, \quad (3.3)$$

$$\|(\Phi^{-n})^*(\mathbf{x})\mathbf{v}_s\| \geq c\lambda^n \|\mathbf{v}_s\|, \quad \|\Phi^{n*}(\mathbf{x})\mathbf{v}_s\| \leq b\lambda^{-n} \|\mathbf{v}_s\|. \quad (3.4)$$

Hyperbolic theory has been generalized by Pesin [22,23] to a more general class of systems referred to as nonuniformly hyperbolic, for which the stable-unstable splitting Eqs. (3.1) and (3.2) hold, while Eqs. (3.3) and (3.4) for the expansion-contraction rates are reformulated in a weaker nonuniform (position-dependent) way. A succinct review of Pesin's theory can be found in Ref. [24].

There is a close relation between chaotic behavior as defined by Eq. (2.2) and hyperbolicity. Equation (2.2) is the basic condition defining a quasi-Anosov diffeomorphism on a submanifold \mathcal{C}_c [15]. Indeed, Mañé has proved that, for two-dimensional compact submanifolds \mathcal{C}_c , the property expressed by Eq. (2.2) implies that the diffeomorphism Φ is also Anosov [15], and therefore \mathcal{C}_c admits a hyperbolic structure invariant under Φ . This property is strictly valid for two-dimensional manifolds, while in three or more dimensions the situation is more complex [15]. For two-dimensional systems, however, the Mañé theorem implies that chaotic area-preserving diffeomorphisms are hyperbolic once restricted to an invariant chaotic region, although hyperbolicity cannot be extended over all the phase space. This result is of fundamental importance in the study of chaotic dynamical systems restricted to the chaotic region (which turns out to be the most important case in the study of chaotic systems and of stretching dynamics) because it enables us to apply the powerful apparatus of hyperbolic theory to physically interesting problems associated with Poincaré maps of Hamiltonian systems or with models of 2D incompressible flows. The result obtained by Mañé holds for compact submanifolds. In cases where compactness is lost, the splitting of the tangent space expressed by Eqs. (3.1) and (3.2) still holds, but the bounds for the rate of expansion and contraction along the unstable and stable vector sub-bundles remain an open problem. For the purposes of the present article, this result is sufficient to constitute the fundamental starting point for the construction of a geometric invariant theory.

The relationships between chaotic behavior and hyperbolicity are referred to by some authors [25] as Ruelle's chaotic hypothesis [26], which has been interpreted by Gallavotti and Cohen as follows: "a chaotic mechanical system can be regarded for practical purposes as a topological mixing system" [27], i.e., as a mixing Anosov system. Though related

primarily to the analysis of dissipative dynamics with many degrees of freedom and aimed at the analysis of their Sinai-Ruelle-Bowen (SRB) measures [29], the observation put forward by Gallavotti can be applied to 2D differentiable area-preserving systems. Borrowing a highlighting analogy due to Gallavotti [27], we can state that hyperbolicity for 2D area-preserving differentiable dynamics provides a model-independent theoretical framework to describe and understand their global geometric and measure-theoretical properties (namely, the w measure discussed in Sec. IV) just as Boltzmann's ergodic hypothesis led to the success of equilibrium statistical mechanics.

In 2D systems both \mathcal{E}_x^u and \mathcal{E}_x^s are one-dimensional vector subspaces. The numerical evaluation of a vector basis for the unstable vector subspace \mathcal{E}_x^u can be obtained by enforcing the concept of asymptotic directionality [28], by considering the sequence of unstable eigenvectors $\mathbf{e}_n^u(\mathbf{x})$ of the differential $\Phi^{n*}(\Phi^{-n}(\mathbf{x}))$

$$\Phi^{n*}(\Phi^{-n}(\mathbf{x}))\mathbf{e}_n^u(\mathbf{x}) = \omega_n(\mathbf{x})\mathbf{e}_n^u(\mathbf{x}). \quad (3.5)$$

Indeed, if a diffeomorphism is hyperbolic in \mathcal{C} then the sequence of eigenvectors $\mathbf{e}_n^u(\mathbf{x})$ eventually exists [30] with $|\omega_n(\mathbf{x})| \rightarrow \infty$ and converges (in direction) to a limit eigenvector $\mathbf{e}^u(\mathbf{x})$ spanning \mathcal{E}_x^u . The same property holds for the stable vector sub-bundle by considering Φ^{-1} instead of Φ , thus obtaining the basis $\{\mathbf{e}^s(\mathbf{x})\}$. An alternative way of computing $\mathbf{e}^u(\mathbf{x})$ makes use of the homeomorphism between $SL(2, \mathbb{R})$ and real-valued Möbius transforms (as discussed in the Appendix).

The invariant hyperbolic structure makes it possible to decouple the stretching dynamics in terms of a strictly multiplicative process. For two-dimensional systems, the elongation exponent after n iterations at point \mathbf{x} can be defined as

$$a_n(\mathbf{x}) = \ln \lambda_e^{(n)}(\mathbf{x}) = \ln \|\Phi^{n*}(\mathbf{x})\mathbf{e}^u(\mathbf{x})\|, \quad (3.6)$$

where $\lambda_e^{(n)}(\mathbf{x})$ defines the elongation. Contrary to the definition of the stretchings $\lambda^{(n)}(\mathbf{x}, \mathbf{v}/\|\mathbf{v}\|)$, the elongation $\lambda_e^{(n)}(\mathbf{x})$ is, strictly speaking, a field, i.e., depends exclusively on the position \mathbf{x} (for fixed n). This definition of elongations has been already discussed by several authors [28,31], and is applied in Sec. VII.

IV. GEOMETRIC STRUCTURE OF THE UNSTABLE FOLIATION

Given the unstable vector sub-bundle $\{\mathbf{e}^u(\mathbf{x})\}_{\mathbf{x} \in \mathcal{C}}$, it is possible to define the dynamical system generated by $\mathbf{e}^u(\mathbf{x})$,

$$\frac{d\mathbf{x}_w(p)}{dp} = \mathbf{e}^u(\mathbf{x}_w(p)), \quad (4.1)$$

starting from $\mathbf{x}_w(p=0) = \mathbf{x}_o \in \mathcal{C}$. In Eq. (4.1) the parameter p plays the role of a generic parametrization of the trajectories generated by the unstable sub-bundle. Equation (4.1) makes sense since by hypothesis $\mathbf{e}^u(\mathbf{x}_w(p))$ is continuous along the trajectories, and the corresponding dynamical system is referred to as the w system associated with the Poincaré map Φ [33].

Consider a generic point $\mathbf{x}_o \in \mathcal{C}$, and the solution $\mathbf{x}_w(p; \mathbf{x}_o)$ of Eq. (4.1) for $p \in [0, p_1]$ passing as initial condition ($p=0$) through \mathbf{x}_o . This solution defines a curve arc $\gamma_{\mathbf{x}_o}^+(p_1)$ on \mathcal{C} . Similarly, by exchanging p with $-p$ and integrating from 0 to $-p_1$, it is possible to define a new curve arc $\gamma_{\mathbf{x}_o}^-(p_1)$. These two curve arcs can be joined together to form a single curve arc $w_{\mathbf{x}_o}^u(p_1) = \gamma_{\mathbf{x}_o}^-(p_1) \cup \gamma_{\mathbf{x}_o}^+(p_1)$ passing through \mathbf{x}_o . By definition $w_{\mathbf{x}_o}^u(p_1)$ is continuous and differentiable at \mathbf{x}_o and may be referred to as a local unstable leaf at \mathbf{x}_o . An important property of the local unstable leaves of the w system is their invariance with respect to Φ : the image $\Phi(w_{\mathbf{x}_o}^u(p_1))$ of $w_{\mathbf{x}_o}^u(p_1)$ through Φ is a local unstable leaf, the solution of Eq. (4.1) passing through $\Phi(\mathbf{x}_o)$. This result stems from the invariance of the unstable sub-bundle with respect to the differential Φ^* . Because of the expanding properties of Φ^* along the unstable sub-bundle, a local unstable leaf $w_{\mathbf{x}_o}^u(\mathbf{x}_o)$ for $p_1 \rightarrow \infty$ becomes unbounded in length and space filling on \mathcal{C} in the sense that it is dense on \mathcal{C} . As a result, it is possible to define a global unstable leaf at a generic point $\mathbf{x}_o \in \mathcal{C}$ as the limit of $w_{\mathbf{x}_o}^u(p_1)$ for $p_1 \rightarrow \infty$, or equivalently as the limit for $n \rightarrow \infty$ of the sequence of integral manifolds $\{\Phi^n(w_{\Phi^{-n}(\mathbf{x}_o)}^u(p_1))\}$. We shall use the notation $w_{\mathbf{x}_o}^u$ to indicate such a global unstable leaf passing through \mathbf{x}_o . The family of all the distinct global unstable leaves for $\mathbf{x}_o \in \mathcal{C}$ is referred to as the invariant unstable foliation $\mathcal{F}_u = \{w_{\mathbf{x}_o}^u\}_{\mathbf{x}_o \in \mathcal{C}}$ of Φ in \mathcal{C} .

In particular, if \mathbf{x}_p is a hyperbolic fixed (periodic) point of Φ , the integral manifold $w_{\mathbf{x}_p}^u(p_1)$ corresponds to the local unstable manifold $\mathcal{W}_{loc}^u(\mathbf{x}_p)$ of \mathbf{x}_p defined in dynamical system theory [18],

$$\begin{aligned} \mathcal{W}_{loc}^u &= \{\mathbf{x} \in U_\varepsilon \mid \Phi^{-n}(\mathbf{x}) \rightarrow \mathbf{x}_p \text{ as } n \rightarrow \infty \\ &\text{and } \Phi^{-n}(\mathbf{x}) \in U_\varepsilon \quad \forall n \geq 0\}, \end{aligned} \quad (4.2)$$

and the global unstable manifold $\mathcal{W}^u(\mathbf{x}_p)$, defined as the union of the images of $\mathcal{W}_{loc}^u(\mathbf{x}_p)$ through Φ^n ,

$$\mathcal{W}^u(\mathbf{x}_p) = \bigcup_{n \geq 0} \Phi^n(\mathcal{W}_{loc}^u(\mathbf{x}_p)), \quad (4.3)$$

coincides with the leaf $w_{\mathbf{x}_p}^u$ of the unstable foliation.

Since \mathcal{F}_u is transitive in \mathcal{C} (i.e., each leaf of the unstable foliation fills \mathcal{C} densely), and since two leaves passing in a neighborhood of a point \mathbf{x} possess close tangent vectors (because the vector subspaces $\{\mathcal{E}_x^u\}$ are continuous almost everywhere in \mathcal{C}), a generic leaf of the unstable foliation is representative of the foliation itself. More precisely, a class of equivalence of the leaves of \mathcal{F}_u can be defined in such a way that all the leaves belong to the same equivalence class. The equivalence between leaves of the unstable foliation is graphically depicted in Figs. 1(a) and 1(b) in the case of the standard map ($\kappa=2$). Figure 1(a) shows a portion of $w_{\mathbf{x}_o}^u$ starting from a randomly chosen point $\mathbf{x}_o \in \mathcal{C}$ (the chaotic region is dotted), while Fig. 1(b) shows a portion of the unstable manifold of the hyperbolic fixed point $\mathbf{x}_p = (0, \frac{1}{2})$. For the purposes of a global geometric theory of 2D differentiable area-preserving dynamics, it is immaterial to ana-

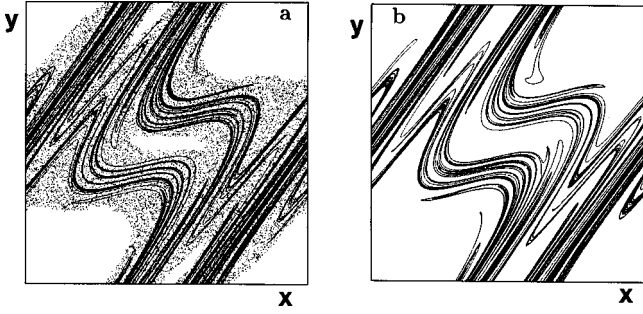


FIG. 1. (a) Chaotic region \mathcal{C} (dotted) and a portion of an integral manifold (continuous line) obtained by integrating Eq. (4.1) starting from a randomly chosen initial point within \mathcal{C} . (b) Portion of the unstable manifold of the fixed point $(0, \frac{1}{2})$. The dynamical system is the standard map Eq. (2.3) with $\kappa=2$.

lyze the properties of a generic leaf of the unstable foliation or the global unstable manifold of some particular hyperbolic periodic point since both the manifolds contain exactly the same amount of information on the invariant dynamics and global geometry of the system. This observation is useful especially in the analysis of fluid mixing systems since it indicates that a generic leaf of \mathcal{F}^u (and not only the unstable manifold associated with some particular hyperbolic periodic points) is the fundamental template for the asymptotic evolution of material lines and partially mixed structures advected by the flow [34].

As can be argued from visual inspection of Fig. 1, the spatial distributions of the unstable leaves within a chaotic region is highly nonhomogeneous. This spatial heterogeneity has been already observed in the evolution of material lines advected by laminar chaotic flows [5] and is of primary relevance for the quantitative modeling of the interfacial phenomena controlled by the structure of material lines (a closed material line is the boundary of a fluid element). A typical example of such problems is reaction-diffusion kinetics in laminar chaotic flows in the limit of large Thiele moduli (i.e., for very fast reactions) and large Péclet numbers (i.e., negligible diffusion) [35].

For the reason stated above, it is interesting to investigate the statistical and measure-theoretical properties of the leaves of the unstable foliation both within the framework of a global theory of dynamical systems and for its applications to fluid mixing and mechanical models. Let us frame this project in a quantitative way. Henceforth we shall regard $\mathbf{e}^u(\mathbf{x})$ in Eq. (4.1) as unit vectors (i.e., $\|\mathbf{e}^u(\mathbf{x})\|=1$), so that the parameter p corresponds to the curvilinear abscissa parametrizing the unstable leaves of \mathcal{F}^u . The measure-theoretical (space-filling) properties of \mathcal{F}^u can be addressed by analyzing the inter-material length density $\rho_w(\mathbf{x})$ (since 2D systems are considered), i.e., the normalized pointwise length distribution of a generic leaf of \mathcal{F}^u . In laminar chaotic flows this quantity has a straightforward physical meaning as it provides a pointwise description of the multiplicative formation of striations due to the mixing protocol. Let μ_w be the associated measure, referred to as the w -invariant measure (or simply as the w -measure). Because of the invariance of \mathcal{F}^u with respect to Φ , it follows that the density $\rho_w(\mathbf{x})$ (if it exists) and the measure μ_w are respectively the invariant density and measure associated with the dynamical system Eq. (4.1). Under the assumption of the existence of a density

(this point is analyzed thoroughly in Sec. V), it follows from the continuity equation that the w density satisfies the equation

$$\nabla \cdot [\rho_w(\mathbf{x})\mathbf{e}^u(\mathbf{x})] = 0. \quad (4.4)$$

In a similar way, if $\phi_p^w(\mathbf{x})$ is the phase flow associated with Eq. (4.1), the w measure satisfies the equation

$$\mu_w(B) = \mu_w((\phi_p^w)^{-1}(B)), \quad (4.5)$$

for any measurable set $B \subseteq \mathcal{C}$, i.e., is invariant under the flow associated with Eq. (4.1). The analysis developed for the unstable foliation can be extended in a straightforward way to the stable foliation \mathcal{F}^s by simply considering the integral manifolds associated with the stable vector sub-bundle $\{\mathbf{e}^s(\mathbf{x})\}$.

In the case of hyperbolic systems given by Eqs. (2.5) and (2.6), the unstable vector sub-bundle $\{\mathbf{e}^u(\mathbf{x})\}$ can be obtained analytically [13], and is given by $\mathbf{e}^u(\mathbf{x}) = [\mathcal{H}^*(\mathbf{x})]^{-1}\boldsymbol{\varepsilon}^u$, where $\boldsymbol{\varepsilon}^u$ is the unstable eigenvector of the matrix \mathbf{B}

$$[\mathbf{B}\boldsymbol{\varepsilon}^u = \lambda_u\boldsymbol{\varepsilon}^u, \lambda_u = (3 + \sqrt{5})/2, \boldsymbol{\varepsilon}^u = (\varepsilon_1^u, \varepsilon_2^u)' = (1, \lambda_u - 1)'].$$

Where the diffeomorphism \mathcal{H} is given by the standard map, the integral manifolds of the unstable foliation can be expressed in closed form. For w_{x_0} the integration of Eq. (4.1) yields

$$x = x_0 \pm \left[\frac{\varepsilon_1^u(y - y_0)}{\varepsilon_2^u - \varepsilon_1^u} + \frac{\kappa}{2\pi} [\sin(2\pi y) - \sin(2\pi y_0)] \right]. \quad (4.6)$$

By enforcing the identity $\nabla \cdot \{[\mathcal{H}^*(\mathbf{x})]^{-1}\boldsymbol{\varepsilon}^u\} = 0$, it readily follows from Eq. (4.4) that the w density $\rho_w(\mathbf{x})$ exists and is given by

$$\rho_w(\mathbf{x}) = C \|[\mathcal{H}^*(\mathbf{x})]^{-1}\boldsymbol{\varepsilon}^u\|, \quad (4.7)$$

where C is the normalization constant. As a consequence, the w measure for hyperbolic diffeomorphisms of the torus [32] is absolutely continuous with respect to the Lebesgue measure. The analysis of the structure of the w -invariant measure for generic 2D chaotic area-preserving systems is developed in the following sections.

V. STATIONARY MEASURE OF THE UNSTABLE FOLIATION

In order to determine an analytic expression for the w -invariant measure of a generic 2D area-preserving diffeomorphism it is convenient to apply a constructive process following the advection of a material line iteration by iteration. Let γ_0 be a curve arc (such that $\gamma_0 \cap \mathcal{C}$ is the union of a discrete number of curve arcs of nonzero length) and $\gamma_n = \Phi^n(\gamma_0)$ its image through Φ^n . The statistical properties of γ_n can be addressed by analyzing the intermaterial length density $\rho_w^{(n)}(\mathbf{x})$ at iteration n .

The density $\rho_w^{(n)}(\mathbf{x})$ and the associated measure $\mu_w^{(n)}$ can be obtained numerically by tracking the curves γ_n and by box counting the length fraction falling within each box of the covering of \mathcal{C} . By invoking the asymptotic equivalence

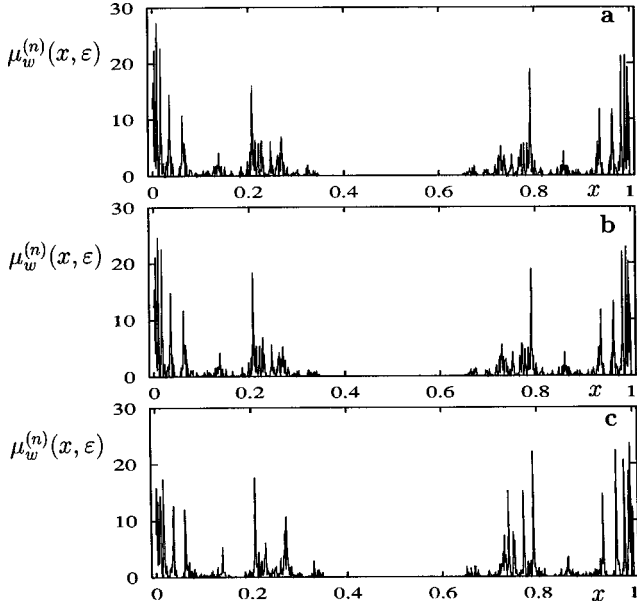


FIG. 2. Intersection box measure $\mu_w^{(n)}(x, \varepsilon)$ vs x at $y = \frac{1}{2}$ for the standard map at $\kappa=2$ ($\varepsilon = 5 \times 10^{-4}$). (a) Filament evolution, $n = 12$, (b) filament evolution, $n = 14$, (c) generic leaf of the invariant unstable foliation \mathcal{F}^u .

between advected lines and the leaves of the unstable foliation \mathcal{F}^u , the sequence of measures $\mu_w^{(n)}$ converges in the limit of $n \rightarrow \infty$ towards a stationary measure μ_w (w measure), which is the invariant measure of the dynamical system, Eq. (4.1), and the stationary pointwise length distribution of a generic material line stretched and folded by the Poincaré map Φ . This phenomenon is shown in Fig. 2 by taking a section along $y = y_c$ and plotting the intersection box measures $\mu_w^{(n)}(x_i, \varepsilon)$ representing the fraction of intersections falling in an interval $[x_i, x_i + \varepsilon)$ along y_c for a filament evolution ($n = 12, 14$) and for a generic leaf of the unstable foliation \mathcal{F}^u . These two measures have been obtained from a box counting of the intersections within the intervals of a given partition of $y = y_c$. The dynamical system considered is the standard map Eq. (2.3) at $\kappa=2$, $y_c = \frac{1}{2}$. These box measures are normalized as $\sum_i \mu_w^{(n)}(x_i, \varepsilon) \varepsilon = 1$. Apart from minor effects due to tangencies between filament evolution (invariant manifolds) with $y = y_c$, the box counting of intersections is equivalent to the box counting of the length content.

In order to obtain an analytical approximation for $\rho_w^{(n)}(\mathbf{x})$ at iteration n , it is convenient (and conceptually more elegant) to analyze the measure-theoretical properties of Eq. (4.1) by enforcing asymptotic directionality, Eq. (3.5). This will provide a deeper insight into the functional form of $\rho_w^{(n)}(\mathbf{x})$ than the purely numerical tracking and box-counting of a material line. Let us set $\mathbf{A}^{(n)} = \Phi^{n*}(\Phi^{-n}(\mathbf{x})) = (A_{ij}^{(n)})$. For sufficiently large n , within the chaotic region \mathcal{C}

$$\text{tr}[\Phi^{n*}(\Phi^{-n}(\mathbf{x}))] = A_{11}^{(n)} + A_{22}^{(n)} = \lambda_n^u + 1/\lambda_n^u = \lambda_n^u + o(n),$$

$$\mathbf{x} \in \mathcal{C}, \quad (5.1)$$

where $o(n)$ is a quantity tending (exponentially) to zero for $n \rightarrow \infty$. Within this approximation (which proves to be exact

for $n \rightarrow \infty$), the eigenvector $\mathbf{e}_n^u(\mathbf{x}) = (e_{n,1}^u, e_{n,2}^u)^t$ can be obtained from the solution of the equation

$$-A_{22}^{(n)} e_{n,1}^u + A_{12}^{(n)} e_{n,2}^u = 0 \quad (5.2)$$

or, equivalently,

$$A_{21}^{(n)} e_{n,1}^u - A_{11}^{(n)} e_{n,2}^u = 0. \quad (5.3)$$

A non-normalized basis for \mathcal{E}_x^u can therefore be approximated by

$$\hat{\mathbf{e}}_n^u(\mathbf{x}) = (A_{12}^{(n)}, A_{22}^{(n)})^t \quad (5.4)$$

or, equivalently, by

$$\hat{\mathbf{e}}_n^u(\mathbf{x}) = (A_{11}^{(n)}, A_{21}^{(n)})^t. \quad (5.5)$$

The reason why two different approximations, Eqs. (5.4) and (5.5), are obtained is related to hyperbolicity. The differential $\mathbf{A}^{(n)} = \Phi^{n*}(\Phi^{-n}(\mathbf{x}))$ possesses entries which diverge exponentially as n increases and is subjected to the condition $\det(\mathbf{A}^{(n)}) = 1$. Therefore, if $m_n \sim \exp(n\lambda)$ ($\lambda > 0$) indicates the maximum over the entries of $\mathbf{A}^{(n)}$, the normalized matrix $\tilde{\mathbf{A}}^{(n)} = \mathbf{A}^{(n)}/m_n$ admits a determinant exponentially decreasing to zero. This implies that the two column vectors $\mathbf{e}_{n,1}^u = (A_{11}^{(n)}/m_n, A_{21}^{(n)}/m_n)^t$, $\mathbf{e}_{n,2}^u = (A_{12}^{(n)}/m_n, A_{22}^{(n)}/m_n)^t$ forming $\tilde{\mathbf{A}}^{(n)} = (\mathbf{e}_{n,1}^u, \mathbf{e}_{n,2}^u)$ become colinear with each other as n increases, and two different expressions for $\mathbf{e}_n^u(\mathbf{x})$, Eqs. (5.4) and (5.5), are available.

By differentiating the identity $\Phi^n(\Phi^{-n}(\mathbf{x})) = \mathbf{x}$, it follows that

$$\mathbf{A}^{(n)} = \Phi^{n*}(\Phi^{-n}(\mathbf{x})) = [(\Phi^{-n}(\mathbf{x}))^*]^{-1}, \quad (5.6)$$

and the vector $\hat{\mathbf{e}}_n^u(\mathbf{x})$ can therefore be expressed as

$$\hat{\mathbf{e}}_n^u(\mathbf{x}) = \left(-\frac{\partial \Phi_i^{-n}(\mathbf{x})}{\partial x_2}, \frac{\partial \Phi_i^{-n}(\mathbf{x})}{\partial x_1} \right)^t \quad i = 1, 2, \quad (5.7)$$

where $\mathbf{x} = (x_1, x_2)^t$ is a Cartesian coordinate system for the phase manifold and $\Phi_i^{-n}(\mathbf{x})$ the i th component of the map Φ^{-n} . As can be observed from Eq. (5.7), the functions Φ_i^{-n} ($i = 1, 2$) play the role of asymptotic invariant ‘‘stream functions,’’ determining through Eq. (4.1) the invariant properties of the unstable manifolds of Φ in the limit for $n \rightarrow \infty$. The choice of $i = 1, 2$ in Eq. (5.7) determines two different approximations for $\hat{\mathbf{e}}_n^u(\mathbf{x})$ which return a vector colinear to $\mathbf{e}^u(\mathbf{x})$ in the limit of $n \rightarrow \infty$ and are therefore fully equivalent.

Equation (5.7) is the starting point in order to determine an analytic expression for $\rho_w^{(n)}(\mathbf{x})$. Indeed, from Eq. (5.7) it is easy to see that

$$\nabla \cdot \hat{\mathbf{e}}_n^u(\mathbf{x}) = -\frac{\partial^2 \Phi_i^{-n}(\mathbf{x})}{\partial x_1 \partial x_2} + \frac{\partial^2 \Phi_i^{-n}(\mathbf{x})}{\partial x_2 \partial x_1} = 0. \quad (5.8)$$

By definition, the n th approximation $\rho_w^{(n)}(\mathbf{x})$ for the w -invariant density fulfills the continuity equation

$$\nabla \cdot [\rho_w^{(n)}(\mathbf{x}) \mathbf{e}_n^u(\mathbf{x})] = 0, \quad (5.9)$$

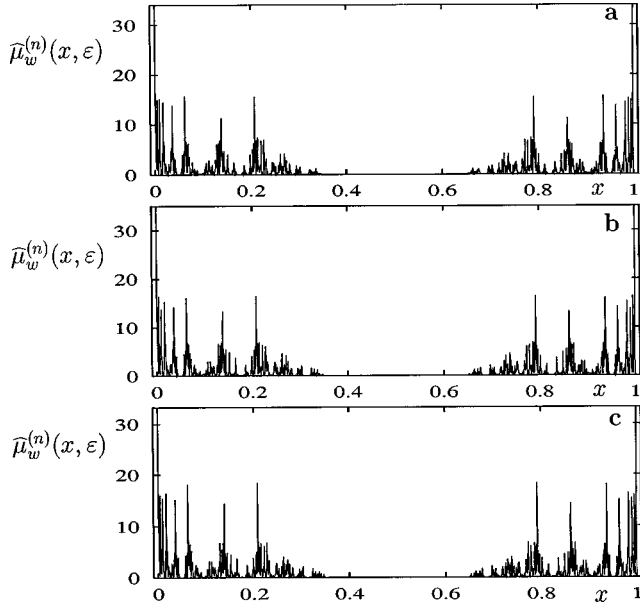


FIG. 3. Normalized sectional box measures $\hat{\mu}_w^{(n)}(x, \varepsilon)$ vs x along the x axis ($\kappa=2$) at $y_c = \frac{1}{2}$ ($\varepsilon = 5 \times 10^{-4}$). (a) $n=9$, (b) $n=10$, (c) $n=11$.

where $\mathbf{e}_n^u(\mathbf{x})$ are colinear with $\hat{\mathbf{e}}_n^u(\mathbf{x})$ and possess unit norm. Equation (5.9) is a continuity equation analogous to Eq. (4.4) with $\rho_w(\mathbf{x})$ replaced by $\rho_w^{(n)}(\mathbf{x})$ and $\mathbf{e}^u(\mathbf{x})$ replaced by $\mathbf{e}_n^u(\mathbf{x})$. Since $\mathbf{e}_n^u(\mathbf{x}) = \hat{\mathbf{e}}_n^u(\mathbf{x}) / \|\hat{\mathbf{e}}_n^u(\mathbf{x})\|$, it follows from Eq. (5.8) that $\nabla \cdot [\|\hat{\mathbf{e}}_n^u(\mathbf{x})\| \mathbf{e}_n^u(\mathbf{x})] = 0$, and therefore the comparison with Eq. (5.9) yields an analytical expression from $\rho_w^{(n)}(\mathbf{x})$:

$$\rho_w^{(n)}(\mathbf{x}) = \text{const} \times \|\hat{\mathbf{e}}_n^u(\mathbf{x})\| + o(n) = \rho_w^{(n)}(\mathbf{x}) = \text{const} \times \|\nabla \Phi_i^{-n}(\mathbf{x})\| + o(n) \quad i=1,2 \quad (5.10)$$

or, equivalently,

$$\rho_w^{(n)}(\mathbf{x}) = \text{const} \hat{\rho}_w^{(n)}(\mathbf{x}) + o(n),$$

$$\hat{\rho}_w^{(n)}(\mathbf{x}) = \left[\left(\frac{\partial \Phi_i^n}{\partial x_1} \right)_{\Phi^{-n}(\mathbf{x})}^2 + \left(\frac{\partial \Phi_i^n}{\partial x_2} \right)_{\Phi^{-n}(\mathbf{x})}^2 \right]^{1/2} \quad i=1,2. \quad (5.11)$$

Equation (5.11) provides a sequence of analytical approximations for $\rho_w(\mathbf{x})$ from which the statistical properties of the measures $\mu_w^{(n)}$ generated from these densities and their convergence properties can be addressed.

For each n , the densities $\rho_w^{(n)}(\mathbf{x})$ are differentiable despite the fact that in the limit for $n \rightarrow \infty$ the sequence of measures $\mu_w^{(n)}$ converges towards a stationary singular measure, as will be discussed in detail in the next section. This phenomenon is illustrated in Fig. 3 by considering the sectional box measures $\hat{\mu}_w^{(n)}(x_i, \varepsilon)$

$$\hat{\mu}_w^{(n)}(x_i, \varepsilon) = C^{(n)} \int_{x_i}^{x_i + \varepsilon} \rho_w^{(n)}(\xi, y_c) d\xi, \quad (5.12)$$

where $C^{(n)}$ is a normalization constant such that

$$\sum_i \hat{\mu}_w^{(n)}(x_i, \varepsilon) \varepsilon = 1,$$

and $\rho_w^{(n)}$ is given by Eq. (5.11), for the standard map Eq. (2.3) at $\kappa=2$, $y_c = \frac{1}{2}$ and $n=9,10,11$.

The analysis of the results shown in Fig. 3 and its comparison with Fig. 2 make it possible to draw the following conclusions. (a) The sequence of approximants $\mu_w^{(n)}$ obtained through Eq. (5.11),

$$\mu_w^{(n)}(\Delta) = \int_{\Delta} \rho_w^{(n)}(\mathbf{x}) d\mathbf{x}, \quad (5.13)$$

where Δ is a Borelian set, converges with sufficient rapidity towards a spatially nonuniform stationary measure. (b) This measure coincides with the box measure obtained from the box counting of the length of a generic material line evolved for a sufficiently long time, or equivalently from the box counting of the pointwise length distribution of a leaf of \mathcal{F}^u .

Indeed, Eqs. (5.10) and (5.11) yield two different sequences of approximants ($i=1,2$) for $\rho_w^{(n)}$. Figures 4(a), 4(c), and 4(e) and Figs. 4(b), 4(d), and 4(f) show, respectively, the two sequences of sectional box measures $\hat{\mu}_w^{(n)}(x, \varepsilon)$ at $y=0.4$ for the standard map $\kappa=2$, evaluated from Eq. (5.11) for $i=1$ and $i=2$. It may be observed that the two approximations both converge towards the same stationary measure although the convergence rate may be different.

Although asymptotic directionality, Eq. (3.5), holds only for points \mathbf{x} belonging to a chaotic region, the final expression for $\rho_w^{(n)}(\mathbf{x})$ Eq. (5.11) can be defined in principle at all the points of the phase manifold. This is indeed a very useful final result in that it implies no *a priori* knowledge of the location of the chaotic region, and deserves further discussion. If \mathcal{C} belongs to a chaotic region, the norm $\|\nabla \Phi_i^{-n}(\mathbf{x})\|$ grows exponentially with n , while if it does not, the sequence $\|\nabla \Phi_i^{-n}(\mathbf{x})\|$ grows more slowly than any exponential and the resulting w density becomes zero at the point for $n \rightarrow \infty$. This phenomenon is depicted in Fig. 5, which shows the log-normal plot of the sectional box-measures evaluated at $y_c = \frac{1}{2}$ for the standard map at $\kappa=2$ ($n=9,10,11$). For this particular parameter value, the standard map exhibits at $y_c = \frac{1}{2}$ a large central region of quasiperiodicity [see Fig. 1(a)] and consequently the n th order approximation of the w measure tends to zero with an exponential rate at all the points in this region.

A. Uniformly hyperbolic systems and convergence of $\mu_w^{(n)}$

This section analyzes the convergence properties of the sequence of approximants $\mu_w^{(n)}$ derived from Eq. (5.11) for the w measure. To this end, toral diffeomorphisms conjugate with a linear map Eq. (2.6) provide a useful model system since an analytic expression for the w -invariant density $\rho_w(\mathbf{x})$, Eq. (4.2), is available for this class of systems.

For toral diffeomorphism Eq. (2.6), the matrix $\mathbf{A}^{(n)}$ defined in Sec. V attains the form

$$\mathbf{A}^{(n)} = \Phi^{n*} [\Phi^{-n}(\mathbf{x})] = [\mathcal{H}^*(\mathbf{x})]^{-1} \mathbf{B}^n [(\mathcal{H}^{-1})^*(\mathbf{y})]_{\mathbf{y} = \mathbf{B}^{-n} \mathcal{H}(\mathbf{x})} \quad (5.14)$$

obtained by making use of the identity Eq. (5.6). Let us indicate with h_{ij} , k_{ij} , and B_{ij}^n , respectively, the entries of

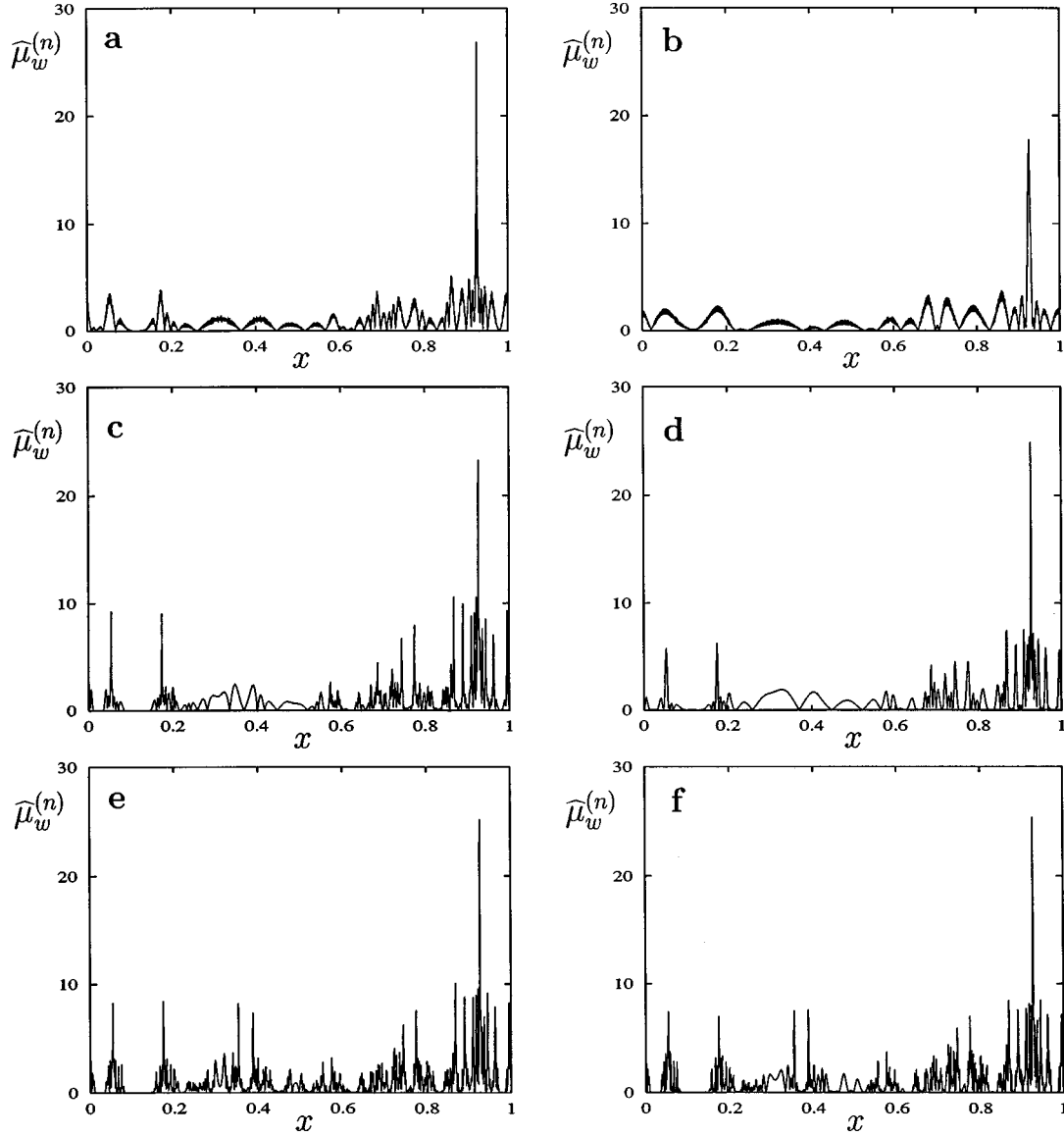


FIG. 4. Normalized sectional box measures $\hat{\mu}_w^{(n)}(x, \varepsilon)$ vs x along the x axis ($\kappa=2$) at $y_c=0.4$ ($\varepsilon=5 \times 10^{-4}$) evaluated from the two different approximations of $\hat{\rho}_w^{(n)}(\mathbf{x})$, Eq. (5.11). (a) $n=5, i=1$, (b) $n=5, i=2$, (c) $n=7, i=1$, (d) $n=7, i=2$, (e) $n=10, i=1$, (f) $n=10, i=2$.

$[\mathcal{H}^*(\mathbf{x})]^{-1}$, $[(\mathcal{H}^{-1})^*(\mathbf{y})]_{\mathbf{y}=\mathbf{B}^{-n}\mathcal{H}(x)}$, and \mathbf{B}^n . By applying Eq. (5.11), the n th order approximation for the w density $\rho_w^{(n)}(\mathbf{x})$ attains the form

$$\hat{\rho}_w^{(n)} = [(A_{1i}^{(n)})^2 + (A_{2i}^{(n)})^2]^{1/2}, \quad i=1,2, \quad (5.15)$$

where

$$\begin{aligned} A_{12}^{(n)} &= h_{11}(B_{11}^n k_{1i} + B_{12}^n k_{2i}) + h_{12}(B_{21}^n k_{1i} + B_{22}^n k_{2i}), \\ A_{22}^{(n)} &= h_{21}(B_{11}^n k_{1i} + B_{12}^n k_{2i}) + h_{22}(B_{21}^n k_{1i} + B_{22}^n k_{2i}), \quad i=1,2. \end{aligned} \quad (5.16)$$

It therefore follows that

$$\hat{\rho}_w^{(n)} = |B_{21}^n k_{1i} + B_{22}^n k_{2i}| \sqrt{(h_{11}\xi^{(n)} + h_{12})^2 + (h_{21}\xi^{(n)} + h_{22})^2}, \quad (5.17)$$

where [see the Appendix, Eq. (A6)]

$$\xi^{(n)} = \frac{B_{11}^n k_{1i}/k_{2i} + B_{12}^n}{B_{21}^n k_{1i}/k_{2i} + B_{22}^n} = \frac{\varepsilon_1^u}{\varepsilon_2^u} + o(n). \quad (5.18)$$

By substituting Eq. (5.18) into Eq. (5.17), it follows that

$$\rho_w^{(n)}(\mathbf{x}) = C g(\Phi^{-n}(\mathbf{x})) \hat{\rho}_w(\mathbf{x}) + o(n), \quad (5.19)$$

where $\hat{\rho}_w = [(h_{11}\varepsilon_1^u + h_{12}\varepsilon_2^u)^2 + (h_{21}\varepsilon_1^u + h_{22}\varepsilon_2^u)^2]^{1/2} = \|[\mathcal{H}^*(\mathbf{x})]^{-1}\varepsilon^u\|$ is the unnormalized w -invariant density Eq. (4.7), C a normalization constant, and $g(\Phi^{-n}(\mathbf{x}))$ a function of $\Phi^{-n}(\mathbf{x})$ given by

$$g(\Phi^{-n}(\mathbf{x})) = \frac{|B_{21}^n k_{1i} + B_{22}^n k_{2i}|}{|\varepsilon_2^u|}. \quad (5.20)$$

It is clear to see that the right-hand side of Eq. (5.20) is a function solely of $\Phi^{-n}(\mathbf{x})$ since k_{ij} are the entries of

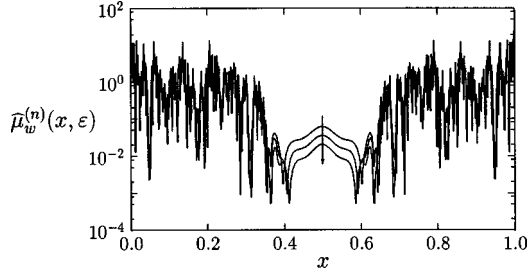


FIG. 5. Log-normal plot of the $\hat{\rho}_w^{(n)}(x, \epsilon)$ vs x along the x axis ($\kappa=2$) at $y_c = \frac{1}{2}$ ($\epsilon = 5 \times 10^{-4}$) for $n=9,10,11$. The arrow indicates increasing values of n .

$(\mathcal{H}^{-1})^*(\mathbf{y})_{\mathbf{y}=\mathbf{B}^n \mathcal{H}(\mathbf{x})} = [\mathcal{H}^*(\Phi^{-n}(\mathbf{x}))]^{-1}$, and the other quantities entering into the definition of g are constant.

Equation (5.19) implies that $\rho_w^{(n)}(\mathbf{x})$ is the product of the smooth, slowly varying function $\hat{\rho}_w(\mathbf{x})$ and of the highly spatially fluctuating term $g(\Phi^{-n}(\mathbf{x}))$. As a consequence of this, the sequence of densities $\rho_w^{(n)}(\mathbf{x})$ does not converge to the invariant w density Eq. (4.7), as shown in Fig. 6 visualizing the pointwise behavior of $\hat{\rho}_w^{(n)}(\mathbf{x})$ along the circumference $x = \frac{1}{2}$, $0 \leq y \leq 1$ at $n=10$ and for \mathcal{H} given by the standard map with $\kappa=6$.

Although the sequence of $\rho_w^{(n)}(\mathbf{x})$ does not converge towards the w -invariant density $\rho_w(\mathbf{x})$, it is straightforward to show that convergence holds in measure. To prove this, let us integrate $\rho_w^{(n)}(\mathbf{x})$ over a ball $\mathcal{B}_x(\epsilon)$ of radius ϵ centered at \mathbf{x} . By applying Eq. (5.19) and enforcing the mean value theorem (for continuous functions) it follows that

$$\begin{aligned} \mu_w^{(n)}(\mathcal{B}_x(\epsilon)) &= C \hat{\rho}_w(\mathbf{x}_\epsilon) \int_{\mathcal{B}_x(\epsilon)} g(\Phi^{-n}(\mathbf{y})) d\mathbf{y} + o(n) \\ &= C \hat{\rho}_w(\mathbf{x}_\epsilon) \int_{\Phi^{-n}(\mathcal{B}_x(\epsilon))} g(\mathbf{y}) d\mathbf{y} + o(n), \end{aligned} \quad (5.21)$$

where \mathbf{x}_ϵ is a point within $\mathcal{B}_x(\epsilon)$. Since Φ is a mixing and g a continuous function, it follows that [36]

$$\lim_{n \rightarrow \infty} \int_{\Phi^{-n}(\mathcal{B}_x(\epsilon))} g(\mathbf{y}) d\mathbf{y} = \mathcal{L}(\mathcal{B}_x(\epsilon)) \langle g \rangle, \quad (5.22)$$

where $\mathcal{L}(\Delta)$ is the Lebesgue measure of the set $\Delta \subseteq \mathcal{T}^2$ and $\langle g \rangle$ the ergodic average of the function g . By substituting this result into Eq. (5.21), it follows that the average density $\bar{\rho}_w^{(n)}(\mathbf{x}, \epsilon)$

$$\begin{aligned} \bar{\rho}_w^{(n)}(\mathbf{x}, \epsilon) &= \frac{1}{\mathcal{L}(\mathcal{B}_x(\epsilon))} \int_{\mathcal{B}_x(\epsilon)} \rho_w^{(n)}(\mathbf{y}), \\ d\mathbf{y} &= \rho_w(\mathbf{x}) + o(n) + O(\epsilon), \end{aligned} \quad (5.23)$$

tends towards the w -invariant density for $n \rightarrow \infty$ and for small ϵ . The result expressed by Eq. (5.23) holds in general for any measurable set centered at \mathbf{x} . This shows that the density $\rho_w^{(n)}(\mathbf{x})$ converges on average, averaged over an arbitrary measurable set, towards the absolutely continuous invariant density $\rho_w(\mathbf{x})$ Eq. (4.6). Because of Eq. (5.23), the box mea-

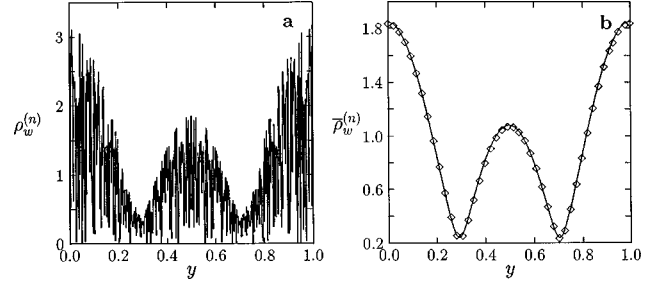


FIG. 6. (a) Pointwise behavior of $\rho_w^{(n)}(\mathbf{x})$ evaluated from Eq. (5.17) along the circumference $x = \frac{1}{2}$, $0 \leq y < 1$ for $n=10$ and for \mathcal{H} given by the standard map ($\kappa=6$). (b) Comparison of $\bar{\rho}_w^{(n)}(\mathbf{x}, \epsilon)$ Eq. (5.23) at $n=10$ numerically evaluated from $\rho_w^{(n)}(\mathbf{x})$ illustrated in Fig. 6(a) and the theoretical expression for $\rho_w(\mathbf{x})$, Eq. (4.7).

asures or the sectional box measures also converge for $n \rightarrow \infty$ if the partition consists of equal boxes. Figure 6 illustrates this result and shows the excellent agreement between $\bar{\rho}_w^{(n)}(\mathbf{x}, \epsilon)$ evaluated from the data of Fig. 6(a) and the w -invariant density Eq. (4.7).

B. Local self-similarity of the w density

This subsection analyzes the local self-similarity of the sequence $\rho_w^{(n)}(\mathbf{x})$ in a neighborhood of a hyperbolic (periodic) point of Φ . The starting point is the definition Eq. (5.10), which can be used in order to obtain a recursive relation for $\rho_w^{(n)}$. To this end, observe that the matrix $\mathbf{A}^{(n)}$ satisfies the relation

$$\mathbf{A}^{(n+1)}(\mathbf{x}) = \Phi^*(\Phi^{-1}(\mathbf{x})) \mathbf{A}^{(n)}(\Phi^{-1}(\mathbf{x})), \quad (5.24)$$

which follows immediately from the definition of

$$\mathbf{A}^{(n)} = [(\Phi^{-n})^*(\mathbf{x})]^{-1} = \Phi^{n*}(\Phi^{-n}(\mathbf{x})) = \prod_{j=1}^n \Phi^*(\Phi^{-j}(\mathbf{x})).$$

Consequently, the vectors $\hat{\mathbf{e}}_n^u(\mathbf{x})$ defined by Eqs. (5.4) and (5.5) satisfy the equation

$$\hat{\mathbf{e}}_{n+1}^u(\mathbf{x}) = \Phi^*(\Phi^{-1}(\mathbf{x})) \hat{\mathbf{e}}_n^u(\Phi^{-1}(\mathbf{x})), \quad (5.25)$$

and the resulting density $\hat{\rho}_w^{(n)}(\mathbf{x}) = \|\hat{\mathbf{e}}_n^u(\mathbf{x})\|$ satisfies the recursive equation

$$\begin{aligned} \hat{\rho}_w^{(n+1)}(\mathbf{x}) &= \|\Phi^*(\Phi^{-1}(\mathbf{x})) \mathbf{e}_n^u(\Phi^{-1}(\mathbf{x}))\| \|\hat{\mathbf{e}}_n^u(\mathbf{x})\| \\ &= \|\Phi^*(\Phi^{-1}(\mathbf{x})) \mathbf{e}_n^u(\Phi^{-1}(\mathbf{x}))\| \hat{\rho}_w^{(n)}(\Phi^{-1}(\mathbf{x})), \end{aligned} \quad (5.26)$$

where $\mathbf{e}_n^u(\mathbf{x})$ is the normalized unit vector colinear with $\hat{\mathbf{e}}_n^u(\mathbf{x})$. Therefore, for \mathbf{y} belonging to an ϵ neighborhood $U_\epsilon(\mathbf{x}_p)$ of a hyperbolic fixed point \mathbf{x}_p and for sufficiently large values of n [such that $\mathbf{e}_n^u(\mathbf{x}) \approx \mathbf{e}^u(\mathbf{x})$], we obtain

$$\hat{\rho}_w^{(n+1)}(\mathbf{x}_p + \mathbf{y}) \approx |\lambda_u| \hat{\rho}_w^{(n)}[\Phi^{-1}(\mathbf{x}_p + \mathbf{y})], \quad (5.27)$$

where λ^u is the unstable eigenvalue of $\Phi^*(\mathbf{x}_p)$ and $||$ indicates the absolute value. Equation (5.27) is derived from Eq. (5.26) by enforcing the continuity of the differential $\Phi^*(\mathbf{x})$. The Taylor expansion of $\Phi^{-1}(\mathbf{x}_p + \mathbf{y})$ in the neighborhood of the fixed point \mathbf{x}_p yields

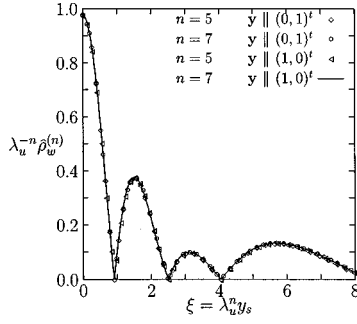


FIG. 7. $\hat{\rho}_w^{(n)}(\xi)/\lambda_u^n$ vs $\xi = \lambda_u^n y^s$ for different orientations and iterations near the hyperbolic fixed point $(0, \frac{1}{2})$ of the standard map ($\kappa=2$).

$$\hat{\rho}_w^{(n+1)}(\mathbf{x}_p + \mathbf{y}) \simeq |\lambda_u| \hat{\rho}_w^{(n)}(\mathbf{x}_p + [\Phi^{-1}(\mathbf{x}_p)]^* \mathbf{y}). \quad (5.28)$$

Equation (5.28) implies that, if $\mathbf{y} \parallel \mathbf{e}^s(\mathbf{x}_p)$ then

$$\hat{\rho}_w^{(n+1)}(\mathbf{x}_p + \mathbf{y}) \simeq |\lambda_u| \hat{\rho}_w^{(n)}(\mathbf{x}_p + \lambda_u \mathbf{y}). \quad (5.29)$$

In the more general case, under the condition that \mathbf{y} is transversal to $\mathbf{e}^u(\mathbf{x}_p)$, we obtain

$$\bar{\rho}_w^{(n+1)}(\mathbf{x}_p + \mathbf{y}) \simeq |\lambda_u|^n \hat{f}_{\mathbf{x}_p}(\mathbf{x}_p + \{[\Phi^{-1}(\mathbf{x}_p)]^*\}^n \mathbf{y}). \quad (5.30)$$

Since \mathbf{x}_p is a fixed (periodic) point, the application of $\{[\Phi^{-1}(\mathbf{x}_p)]^*\}^n$ to \mathbf{y} yields a vector colinear to $\mathbf{e}^s(\mathbf{x}_p)$ in the limit of $n \rightarrow \infty$, i.e.,

$$\begin{aligned} \{[\Phi^{-1}(\mathbf{x}_p)]^*\}^n \mathbf{y} &\simeq (\lambda_u)^n y^s \mathbf{e}^s(\mathbf{x}_p) + (\lambda_u)^{-n} y^u \mathbf{e}^u(\mathbf{x}_p) \\ &\simeq (\lambda_u)^n y^s \mathbf{e}^s(\mathbf{x}_p), \end{aligned} \quad (5.31)$$

where y^s, y^u are the components of \mathbf{y} along the stable and unstable eigenspaces of $\Phi^*(\mathbf{x}_p)$. By collecting together Eqs. (5.30) and (5.31), it follows that for $\mathbf{y} \in U_\varepsilon(\mathbf{x}_p)$

$$\hat{\rho}_w^{(n)}(\mathbf{x}_p + \mathbf{y}) = |\lambda_u|^n f_{\mathbf{x}_p}(\lambda_u^n y^s) + o(n), \quad (5.32)$$

where $f_{\mathbf{x}_p}(\mathbf{x})$ is an invariant function independent of n and y_s is the component of \mathbf{y} along the asymptotic stable direction spanned by $\mathbf{e}^s(\mathbf{x}_p)$ given by $(\Phi^*(\mathbf{x}_p)\mathbf{e}^s(\mathbf{x}_p) = \lambda_u^{-1}\mathbf{e}^s(\mathbf{x}_p))$. Equation (5.32) is the final result expressing the self-similarity of the approximants $\rho_w^{(n)}(\mathbf{x})$ in the neighborhood of a hyperbolic fixed point. A numerical validation of Eq. (5.32) is given in Fig. 7, which shows the graph of $\hat{\rho}_w^{(n)} \times (\xi)/\lambda_u^n$ vs $\xi = \lambda_u^n y^s$ for different values of n , and for different orientations of \mathbf{y} near the hyperbolic fixed point $(0, \frac{1}{2})$ of the standard map ($\kappa=2$). The result derived for hyperbolic fixed points can be extended in straightforward fashion to hyperbolic periodic points of prime period m , which are the fixed points of the $\Phi^m(\mathbf{x})$.

The self-similarity in the neighborhood of periodic points indicates that the structure of the w -invariant measure can be regarded as organized around the skeleton of the hyperbolic periodic points of Φ , which are dense within the chaotic region \mathcal{C} . The global structure of $\rho_w(\mathbf{x})$ is therefore constrained by the local scaling of the w densities expressed by Eq. (5.32). In principle the scaling properties of the w -invariant measure in \mathcal{C} can be derived starting from its

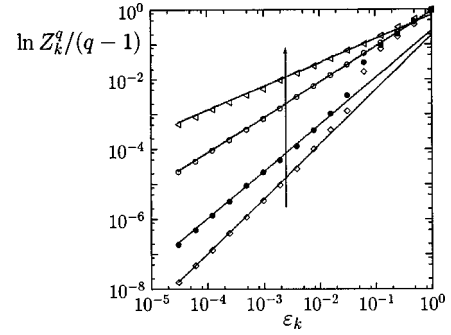


FIG. 8. $\ln Z_k^q / (q-1)$ vs ε_k for the sectional box measures $\hat{\rho}_w^{(n)}(x, \varepsilon)$ of the standard map ($\kappa=2$) at $y_c=0.4$ and $n=11$. The arrow indicates increasing values of q .

local behavior on the dense subset of its hyperbolic periodic points. This phenomenon for the measure-theoretical properties of the unstable foliation is similar to the scaling properties of the invariant measure (the SRB measure) for chaotic dissipative attractors, which can be viewed as organized around the structure of the periodic points [37]. A further discussion of this analogy is developed in Sec. VII. Since each hyperbolic periodic point is characterized by a different scaling factor (eigenvalue), it is to be expected that the resulting w -invariant measure may exhibit highly singular and indeed multifractal features. This topic is examined in the next section.

VI. SINGULAR PROPERTIES OF THE w -INVARIANT MEASURE

This section develops a numerical analysis of the singular structure of the w -invariant measure by considering the structure of its $f(\alpha)$ spectrum and its sign-singularity associated with the orientational properties of the vectors $\hat{\mathbf{e}}_n^u(\mathbf{x})$ defining $\hat{\rho}_w^{(n)}(\mathbf{x})$ through Eq. (5.10).

A. Multifractal properties

In order to investigate the singularity properties of the w measure, the standard multifractal approach is applied [39] by first analyzing the scaling properties of the moments of the normalized sectional box-measures

$$\sum_{i=1}^{N_k} [p_i^{(n)}(\varepsilon_k)]^q \sim \varepsilon_k^{(q-1)\hat{D}(q)}, \quad (6.1)$$

where $p_i^{(n)}(\varepsilon_k)$ is the n th order approximation of the sectional box measure of the i th interval of the partition of size ε_k . The analysis was performed by considering $\varepsilon_k = 2^{-k}$, $k = 1, \dots, 15$.

Figure 8 shows the behavior of the functions $Z_k^q = \{\sum_{i=1}^{N_k} [p_i^{(n)}(\varepsilon_k)]^q\}^{1/(q-1)}$ for some characteristic values of q in the interval $[-10, 10]$, the slope of which in a log-log plot equals the generalized dimension $\hat{D}(q)$ of order q . These data refer to $n=11$, and to a sectional box measure evaluated at $y_c=0.4$ for the standard map at $\kappa=2$. As can be observed, a neat scaling behavior (in the whole range of q) exists over more than three decades of ε_k . Similar results were also obtained for the different values of n and different sections

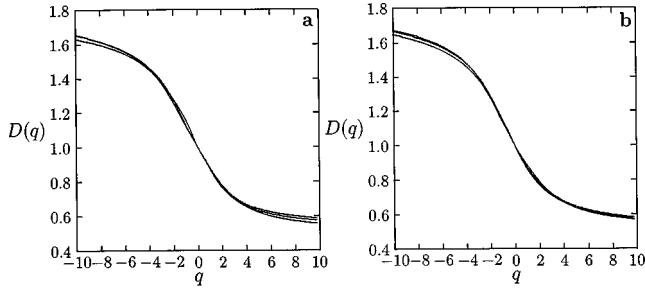


FIG. 9. Spectrum of generalized dimensions of the sectional box measures $\hat{\mu}_w^{(n)}(x, \varepsilon)$ for the standard map ($\kappa=2$). (a) $y_c = \frac{1}{2}$, $n = 10, 11, 12$, (b) $y_c = 0.4$, $n = 10, 11, 12$.

(y_c) considered. These results are summarized in Fig. 9, which shows the spectrum of generalized dimension $\hat{D}(q)$ for $y_c = 0.4$ [Fig. 9(b)] and for $y_c = \frac{1}{2}$ [Fig. 9(a)] at $n = 10, 11, 12$. The $\hat{D}(q)$ curves for different values of n collapse onto a unique invariant curve, thus giving another quantitative confirmation that n th order sectional box measures converge towards an invariant measure (as already shown in qualitative terms in Fig. 2). The comparison of Figs. 9(a) and 9(b) reveals that the $\hat{D}(q)$ spectra for different values of n collapse onto a unique invariant spectrum which is the same for all the different y_c sections analyzed, thus confirming that the simpler analysis of the multifractal properties of sectional box measures provides an insight into the singularity structure of the w measure as a whole. The $f(\alpha)$ spectra corresponding to the $\hat{D}(q)$ curves shown Figs. 9(a) and 9(b) are illustrated in Fig. 10.

The observation that the singularity properties of the w -invariant measure can be inferred from the analysis of sectional box-measures is further supported by the numerical observation that there exists a simple relationship between the spectrum of generalized dimensions $\hat{D}(q)$ evaluated from sectional box measures and the spectrum $D(q)$ evaluated from the w -invariant measure defined on \mathcal{C} as a whole:

$$D(q) = \hat{D}(q) + 1, \quad (6.2)$$

as was to be expected given the meaning of sectional box measures. Figure 11 shows the excellent agreement between $\hat{D}(q)$ and $D(q) - 1$ in the case of the standard map at $\kappa = 2$.

The singular nature of the w -invariant measure seems to be a general feature of 2D area-preserving diffeomorphisms

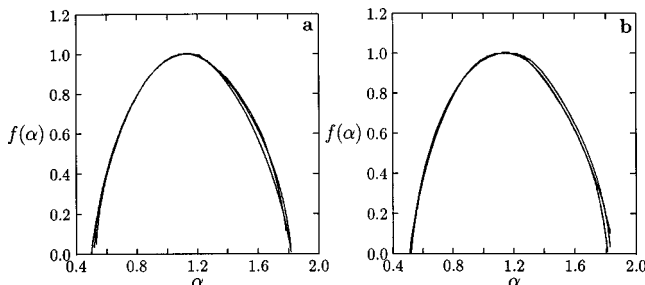


FIG. 10. $f(\alpha)$ spectrum of the sectional box measures $\hat{\mu}_w^{(n)}(x, \varepsilon)$ for the standard map ($\kappa=2$). (a) $y_c = 0.5$, $n = 10, 11, 12$, (b) $y_c = 0.4$, $n = 10, 11, 12$.

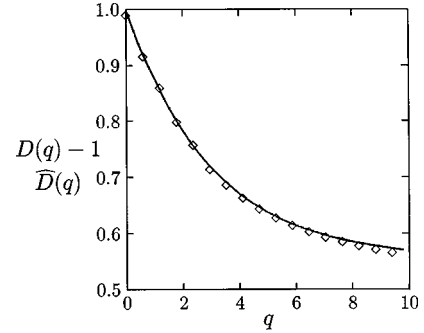


FIG. 11. Comparison between $\hat{D}(q)$ (continuous line) and $D(q) - 1$ (dots) for positive values of q in the case of the standard map at $\kappa = 2$.

which are not conjugate to a linear hyperbolic transformation, although different systems may show rather different spectra of generalized dimensions. A typical case is given by the Poincaré section of the Duffing oscillator Eq. (2.4). Figures 12(a) and 12(b) shows a sectional box measure for this system. A distribution of localized singularities can be observed, Figs. 12(a) and 12(b), although a log-normal plot [Fig. 12(c)] unveils a rich singular structure. Its spectrum of generalized dimensions is shown in Fig. 13. The behavior for negative q values is particularly interesting. From the visual inspection of the sectional box measures the spectrum of generalized dimensions may be expected to be sensitive to the presence of localized zeroes. This observation would explain the sudden elbow obtained for negative values of q near -1 . The solid line in Fig. 13 shows the $\hat{D}(q)$ spectrum (for negative q) associated with localized zeroes $\mu_w^{(n)} \sim \varepsilon^\alpha$ of intensity $\alpha = 1.88$, which fits in well in qualitative terms with the observed behavior for negative q . This observation is of course grounded on purely numerical data.

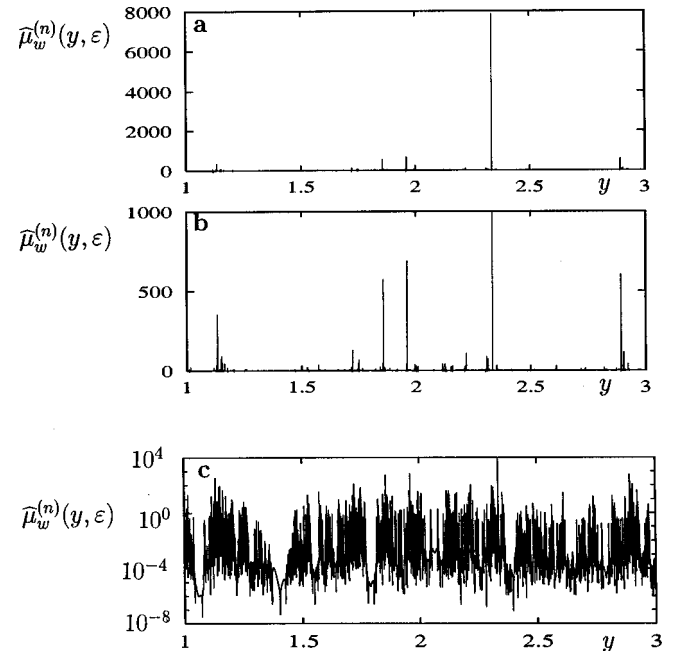


FIG. 12. $\hat{\mu}_w^{(n)}(y, \varepsilon)$ vs $y \in [1, 3]$ at $x = 1$ and $n = 8$ for the Poincaré section of the Duffing oscillator Eq. (2.4) ($\gamma = 0.75$, $\omega = 1.0$). (a) y -axis range $[0, 8000]$, (b) y -axis range $[0, 1000]$, (c) Log-normal plot.

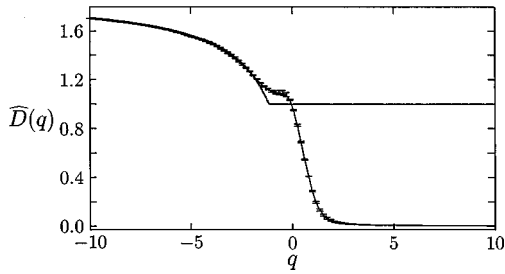


FIG. 13. Spectrum of generalized dimension $\hat{D}(q)$ for the sectional box-measures shown in Fig. 12 (Duffing oscillator), with the corresponding error bars. The bold line, for negative values of q is $\hat{D}(q) = (q-1)^{-1} \max\{q-1, \alpha q\}$ with $\alpha = 1.88$.

Another remarkable property of the w measure arises from the comparison of the singularity structure associated with the stable and unstable foliation of the same dynamical system. Figure 14 compares the $\hat{D}(q)$ spectrum (continuous line) associated with the sectional box measure of the unstable foliation ($y_c = 0.4$, $n = 11$) and the $\hat{D}(q)$ spectrum (dots) associated with the sectional box measures of the stable foliation at $y = 0.4$ for $n = 10$ and $n = 11$ for the standard map at $\kappa = 2$. The spectra of generalized dimensions of these two measures coincide, i.e., the stable and unstable foliation possess the same singularity structure. This phenomenon is a consequence of area preservation in 2D systems. Indeed, if \mathbf{x}_p is a hyperbolic fixed point of Φ^m ($m = 1, 2, \dots$) with the unstable eigenvalue λ_u , it is also a hyperbolic fixed point of Φ^{-m} with the same unstable eigenvalue. On the dense subset of hyperbolic periodic points, the w densities associated with the w systems generated from the vector sub-bundles $\{\mathbf{e}^u(\mathbf{x})\}$, $\{\mathbf{e}^s(\mathbf{x})\}$ therefore possess the same scaling properties (Sec. V B). This observation explains the numerical result shown in Fig. 14.

B. Associated sign-singular measure

In 1992, Ott *et al.* [2] introduced the so-called cancellation exponent in order to characterize the sign-singular properties of the signed measure [40] associated with the magnetic field in fast magnetic dynamos. If ν is a signed measure (a signed measure of a set can take either positive or negative

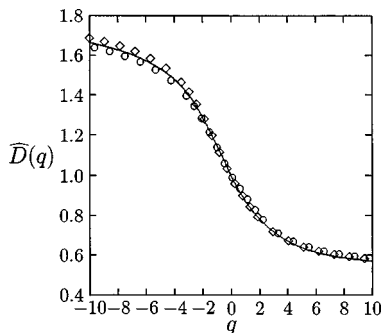


FIG. 14. Comparison between the $\hat{D}(q)$ spectrum (continuous line) associated with the sectional box measures of the unstable foliation ($y_c = 0.4$, $n = 11$) and the $\hat{D}(q)$ spectrum (dots) associated with the sectional box measures of the stable foliation at $y_c = 0.4$ for $n = 10, 11$ for the standard map at $\kappa = 2$.

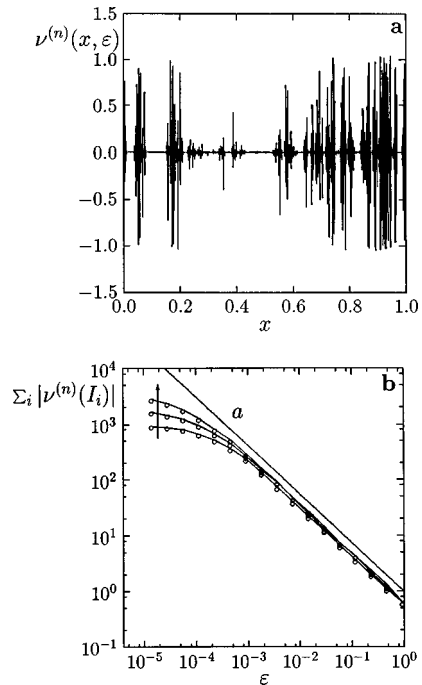


FIG. 15. (a) Signed measure $\nu^{(n)}(x, \varepsilon)$ vs x along the circumference $y_c = 0.4$ (standard map, $\kappa = 2$, $n = 12$), (b) Log-log plot of $\sum_i |\nu^{(n)}(I_i)|$ vs ε for $n = 12, 13, 14$. The arrow indicates increasing values of n . Line (a) is $\sum_i |\nu^{(n)}(I_i)| \sim \varepsilon^{-\kappa_\nu}$ with $\kappa_\nu = 0.83$.

values), ν is said to be sign singular if it changes sign almost everywhere on arbitrarily small lengthscales. For a signed measure, the cancellation exponent may be defined as follows:

$$\kappa_\nu = \limsup_{\varepsilon \rightarrow 0} \frac{\ln \sum_i |\nu(I_i)|}{\ln(1/\varepsilon)}, \quad (6.3)$$

where I_i denotes the i th interval of an ε partition. For a probability measure and for a signed measure with a smooth density $\kappa_\nu = 0$, while $\kappa_\nu > 0$ indicates an oscillation in sign on arbitrarily small lengthscales, i.e., the sign singularity of the measure.

We analyzed the sign-singular properties of the signed measure associated with the normal component of the n th order unstable eigenvectors $\hat{\mathbf{e}}_n^u(\mathbf{x})$ [defining through Eq. (5.10), the w density] along a circumference at $y = y_c$, $0 \leq x \leq 1$ for the standard map defined on the torus. The geometrical meaning of this signed measure is related to the folding of the invariant unstable manifolds and consequently to the folding dynamics in the evolution of partially mixed structures.

Figure 15(a) shows the behavior of $\nu^{(n)}(x_i, \varepsilon)$ for the standard map ($\kappa = 2$) for $n = 12$ and $y_c = 0.4$, indicating persistent oscillations in sign at all length-scales. The sign singular nature of $\nu^{(n)}$ is an asymptotic invariant property. This phenomenon can be highlighted by considering a log-log plot $\sum_i |\nu(I_i)|$ vs ε , as shown in Fig. 15(b) for different values of n . The corresponding slope (in a log-log plot) yields the cancellation exponent $\kappa_\nu^{(n)}$. The sequence $\kappa_\nu^{(n)}$ quickly moves towards a constant value equal to $\kappa_\nu = 0.83$, and the numerical results were obtained by analyzing different sections, i.e., different values of y_c .

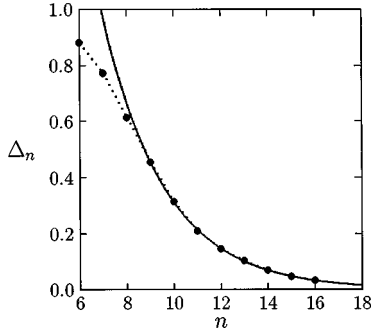


FIG. 16. Distance Δ_n vs n (dots) between the sectional box measures evaluated starting from Eq. (5.10) and Eq. (7.2). The system is the standard map ($\kappa=2$) and $\varepsilon=2^{-9}$, $y_c=\frac{1}{2}$. The solid line is the exponential fitting of the data.

VII. CONNECTION WITH DYNAMIC AND STATISTICAL PROPERTIES

There is a close relation between the w measure and the statistical and pointwise properties characterizing stretching dynamics. Consider again Eq. (5.26). For sufficiently large n , $\mathbf{e}_n^u(\mathbf{x}) = \mathbf{e}^u(\mathbf{x}) + o(n)$ for any $\mathbf{x} \in \mathcal{C}$. Therefore $\|\Phi^*(\Phi^{-1}(\mathbf{x}))\mathbf{e}_n^u(\mathbf{x})\|$ is practically equal to the one-step elongation $\lambda_e^{(1)}(\Phi^{-1}(\mathbf{x}))$ Eq. (3.6), and

$$\hat{\rho}_w^{(n+1)}(\mathbf{x}) = [\lambda_e^{(1)}(\Phi^{-1}(\mathbf{x})) + o(n)] \hat{\rho}_w^{(n)}(\mathbf{x}). \quad (7.1)$$

This result indicates a connection between stretching (elongations) and the expression for the w -invariant density, and suggests the expression

$$\tilde{\rho}_w^{(n)} = C \prod_{j=1}^n \lambda_e^{(1)}(\Phi^{-j}(\mathbf{x})) = C \lambda_e^{(n)}(\Phi^{-n}(\mathbf{x})), \quad (7.2)$$

as another candidate for the n th approximation of $\rho_w(\mathbf{x})$. Of course, as in the case of the expressions Eqs. (5.10) and (5.11), Eq. (7.2) may converge only in measure, i.e., considering its integral over measurable sets. To analyze the convergence properties of Eq. (7.2), let us first consider the case of toral diffeomorphisms Eq. (2.6). For these systems, the elongation $\lambda_e^{(1)}(\Phi^{-n}(\mathbf{x}))$ attains the closed-form expression

$$\lambda_e^{(1)}(\Phi^{-n}(\mathbf{x})) = \exp(n\Lambda) \frac{\|[\mathcal{H}^*(\mathbf{x})]^{-1}\mathbf{e}^u\|}{\|[\mathcal{H}^*(\Phi^{-n}(\mathbf{x}))]^{-1}\mathbf{e}^u\|}, \quad (7.3)$$

where $\Lambda = \ln[(3 + \sqrt{5})/2]$ is the Liapunov exponent. By following the same approach used in Sec. V A to prove the convergence of $\mu_w^{(n)}$, i.e., by applying Eq. (5.22) to the continuous function $g(\mathbf{y}) = 1/\|[\mathcal{H}^*(\mathbf{y})]^{-1}\mathbf{e}^u\|$ entering into Eq. (7.3), we establish that the average density

$$\begin{aligned} \tilde{\rho}_w^{(n)}(\mathbf{x}, \varepsilon) &= \frac{1}{\mathcal{L}(\mathcal{B}_x(\varepsilon))} \int_{\mathcal{B}_x(\varepsilon)} \tilde{\rho}_w^{(n)}(\mathbf{y}) d\mathbf{y} \\ &= C_n \tilde{\rho}_w(\mathbf{x}) + o(n) + O(\varepsilon), \end{aligned} \quad (7.4)$$

converges towards the invariant density Eq. (4.7). A similar result is expected to hold for generic chaotic 2D differentiable area-preserving systems. A quantitative numerical validation of this statement is illustrated in Fig. 16. This

figure shows the distance

$$\Delta_n = \left\{ \int [\hat{\mu}_w^{(n)}(x, \varepsilon) - \tilde{\mu}_w^{(n)}(x, \varepsilon)]^2 dx \right\}^{1/2}$$

between the sectional box-measures evaluated starting from Eq. (5.10), $\hat{\mu}_w(x, \varepsilon)$, and from Eq. (7.2) for the same $\varepsilon = 2^{-9}$ as a function of n . As expected, the distance Δ_n decreases to zero with n , thus supporting the thesis.

We may conclude that the sequence defined by Eq. (7.2) starting from the multiplicative cascade of elongations yields a sequence of approximants for the w density which converges in terms of measure. This result is particularly important since it provides a direct connection between the stretching dynamics and the measure-theoretical properties of the unstable foliation. This result displays some analogies with the corresponding expression for the SRB measure of chaotic dissipative systems as a function of stretching along the unstable directions [29,25]. This analogy is only formal, since the two (SRB and w) measures possess totally different geometric and dynamic meaning. The SRB measure for chaotic attractors is simply the ergodic measure remaining invariant under the map Φ . Its counterpart in 2D area-preserving dynamics restricted to an invariant chaotic submanifold is simply the ergodic measure μ^* associated with the uniform density $\rho^*(\mathbf{x}) = 1/\mathcal{L}(\mathcal{C})$ ($\mathbf{x} \in \mathcal{C}$). Such an invariant measure makes it possible to express time averages of continuous physical observables as ensemble averages of the observables with respect to μ^* [38]. The w -invariant measure is not an ergodic measure for Φ : it is neither invariant under Φ , nor related to the statistical properties of measurable sets transformed by Φ . The w measure is a stationary measure associated exclusively with the geometric structure of the unstable foliation and is the invariant measure [see Eq. (4.5)] for the w system, Eq. (4.1), generated by the normalized unstable vector sub-bundle $\{\mathbf{e}^u(\mathbf{x})\}$.

There is another interesting result emerging from the relation between the w measure and stretching (elongation) dynamics. From Eq. (7.2) it follows that

$$\ln \rho_w^{(n)}(\mathbf{x}) = \ln \tilde{\rho}_w^{(n)}(\mathbf{x}) + \ln C = \sum_{j=1}^n a_1(\Phi^{-j}(\mathbf{x})) + c, \quad (7.5)$$

where C, c are constants independent of \mathbf{x} , i.e., the logarithm of the n th approximant for the w density is the sum of the one-step elongation exponents $a_1(\mathbf{y})$ along a forward trajectory starting from $\Phi^{-n}(\mathbf{x})$. As a result, the variance $\sigma_a^2(n) = \langle [a_n(\mathbf{x}) - \langle a_n \rangle]^2 \rangle = \langle [a_n(\mathbf{x}) - n\Lambda]^2 \rangle$ (Λ is the Liapunov exponent of Φ , and $\langle \cdot \rangle$, the ergodic average within \mathcal{C}), can be expressed as

$$\sigma_a^2(n) = \langle (\ln \rho_w^{(n)}(\mathbf{x}) - \langle \ln \rho_w^{(n)} \rangle)^2 \rangle. \quad (7.6)$$

Equation (7.6) can be used as a criterion in order to make a distinction regarding the structure of the w measure starting from the statistical analysis of the variance of the elongation exponent. For a toral hyperbolic diffeomorphism conjugate to a linear diffeomorphism, the variance $\sigma_a^2(n)$ tends towards a constant value for n tending to infinity [$\lim_{n \rightarrow \infty} \sigma_a^2(n) = \sigma_a^2 \geq 0$]. This corresponds to the fact that the variation of $\ln \rho_w^{(n)}(\mathbf{x})$ is bounded with n , as is to be expected since the w

measure is Lebesgue absolutely continuous and $\rho_w(\mathbf{x})$ is a smooth continuous density. Conversely, for generic hyperbolic diffeomorphisms which are not conjugate to a linear one (such as the standard map or the Poincaré sections of chaotic Hamiltonian–fluid-mixing systems), the variance $\sigma_a^2(n)$ diverges with n [41], and from Eq. (7.6) it follows that this is an indication that the resulting w measure may exhibit a singular structure almost everywhere, as numerically observed in Sec. VI.

VIII. CONCLUDING REMARKS

In this article we have analyzed in detail the properties of the stationary measure associated with the geometric structure of the unstable foliation of 2D area-preserving differentiable dynamics. The convergence in terms of measure of the sequence of analytic approximants Eq. (5.10) has been addressed both analytically and numerically and the relationships between the w measure and the stretching dynamics have been developed Eq. (7.2). In particular, the analogy between the scaling of the variance of the elongation exponents and the singularity structure of the w measure provides a simple numerical test to determine whether the w measure is absolutely continuous [$\lim_{n \rightarrow \infty} \sigma_a^2(n) = \text{const}$] or singular almost everywhere in \mathcal{C} [$\lim_{n \rightarrow \infty} \sigma_a^2(n) = \infty$].

The existence of the w -invariant measure, and the possibility of determining it in a simple way [either by means of Eq. (5.10), (5.11) or through Eq. (7.2)] opens up new horizons in the quantitative characterization of laminar chaotic fluid systems. Since material lines are asymptotically attracted towards the class of equivalence of elements of the unstable foliation \mathcal{F}^u (and indeed this convergence occurs after just a few iterations in most cases), the availability of an analytical expression for the w density makes it possible to develop a more refined model for chaotic laminar mixing. In particular, two problems deserve particular attention in the future: the definition of new mixing indices based on the pointwise properties of partially mixed structures, and the development of coarse-grained models of reaction-diffusion dynamics in chaotic flows. In both cases, the w -invariant measure permits the pointwise quantification of the length distribution of the lamellar structure created by the stretching and folding dynamics (in the limit of negligible diffusion) as well as a deeper understanding of the interfacial phenomena controlled by the coherent structures created by chaotic advection.

APPENDIX: HYPERBOLICITY AND REAL MÖBIUS TRANSFORMS

The group $\text{SL}(2, \mathbb{R})$ is isomorphic to the group of real-valued Möbius transforms. With a matrix $\mathbf{B} \in \text{SL}(2, \mathbb{R})$,

$$\mathbf{B} = \begin{pmatrix} a & b \\ c & d \end{pmatrix}, \quad (\text{A1})$$

($ad - bc = 1$), the linear rational transform

$$f_B(z) = \frac{az + b}{cz + d}, \quad z \in \mathbb{R}, \quad (\text{A2})$$

may be associated. Conversely, to any nondegenerate rational transform $f_B(z) = (\alpha z + \beta)/(\gamma z + \delta)$ (i.e., to any linear rational transform which does not reduce to a constant, which implies $\alpha\delta - \beta\gamma \neq 0$), an element \mathbf{B} of $\text{SL}(2, \mathbb{R})$ may be defined as

$$\mathbf{B} = \frac{1}{\alpha\delta - \beta\gamma} \begin{pmatrix} \alpha & \beta \\ \gamma & \delta \end{pmatrix}. \quad (\text{A3})$$

By defining the application $h: \mathbb{R}^2 \rightarrow \mathbb{R}$ transforming $\mathbf{x} = (x_1, x_2)^t$ into the real number $h(\mathbf{x}) = x_1/x_2$, it follows that

$$h \circ \mathcal{B} = f_B \circ h, \quad (\text{A4})$$

where $\mathcal{B}(\mathbf{x}) = \mathbf{B}\mathbf{x}$ is the linear transform generated by the matrix \mathbf{B} . If the matrix $\mathbf{B} \in \text{SL}(2, \mathbb{R})$ is hyperbolic (i.e., admits real distinct eigenvalues), the corresponding Möbius transform (A2) admits two real fixed points z^u, z^s . The stable point is $z^s = h(\boldsymbol{\varepsilon}^u)$ and the unstable point is $z^u = h(\boldsymbol{\varepsilon}^s)$, $\boldsymbol{\varepsilon}^u$ and $\boldsymbol{\varepsilon}^s$ being the basis vectors spanning the unstable and stable eigenspaces of the matrix \mathbf{B} . This result is a straightforward consequence of Eq. (A4). Indeed, if $\boldsymbol{\varepsilon}$ is an eigenvector of \mathbf{B} ($\mathbf{B}\boldsymbol{\varepsilon} = \lambda\boldsymbol{\varepsilon}$), by applying Eq. (A4) it follows that

$$f_B[h(\boldsymbol{\varepsilon})] = h[\mathcal{B}(\boldsymbol{\varepsilon})] = h(\lambda\boldsymbol{\varepsilon}) = h(\boldsymbol{\varepsilon}), \quad (\text{A5})$$

i.e., $h(\boldsymbol{\varepsilon})$ is a fixed point of f_B . Consider the unstable eigenvector $\boldsymbol{\varepsilon}^u = (\boldsymbol{\varepsilon}_1^u, \boldsymbol{\varepsilon}_2^u)^t$ associated with the unstable eigenvalue λ^u ($|\lambda^u| > 1$). By definition, $c\boldsymbol{\varepsilon}_1^u + d\boldsymbol{\varepsilon}_2^u = \lambda^u \boldsymbol{\varepsilon}_2^u$, i.e., $ch(\boldsymbol{\varepsilon}^u) + d = \lambda^u$. The derivatives of $f_B(z)$ equal $1/(cz + d)^2$, and therefore $f'_B[h(\boldsymbol{\varepsilon}^u)] = (\lambda^u)^{-2} < 1$, which shows that $h(\boldsymbol{\varepsilon}^u)$ is a stable fixed point. Moreover, the sequence $\{z_n\}$ of the iterates of $f_B(z)$, $z_{n+1} = f_B(z_n)$ starting from any initial point $z_o \neq h(\boldsymbol{\varepsilon}^s)$ converges for $n \rightarrow \infty$ towards $h(\boldsymbol{\varepsilon}^u)$.

The Möbius transform associated with a hyperbolic linear diffeomorphism therefore provides a simple way to compute its invariant orientational properties (i.e., the unstable subspaces). In particular, this analysis proves, as a corollary, that if $\mathbf{B}^n = (B_{ij}^n)$ is the n th power of a hyperbolic matrix $\mathbf{B} \in \text{SL}(2, \mathbb{R})$, then for any $z_o \neq h(\boldsymbol{\varepsilon}^s)$ the limit

$$\lim_{n \rightarrow \infty} \frac{B_{11}^n z_o + B_{12}^n}{B_{21}^n z_o + B_{22}^n} = \frac{\boldsymbol{\varepsilon}_1^u}{\boldsymbol{\varepsilon}_2^u}, \quad (\text{A6})$$

holds, which is Eq. (5.18).

The analysis can be extended to 2D nonlinear diffeomorphisms $\Phi(\mathbf{x})$. In this case, a Möbius transform $f_{\Phi^*(\mathbf{x})}(z)$ is

associated with the differential $\Phi^*(\mathbf{x})$. The orientational properties [i.e., a basis $\mathbf{e}^u(\mathbf{x}) = (e_1^u(\mathbf{x}), e_2^u(\mathbf{x}))^t$] for the unstable vector space \mathcal{E}_x^u of Φ are recovered by considering the composition

$$F_x^{(n)}(z) = f_{\Phi^*}(\Phi^{-1}(\mathbf{x})) \circ f_{\Phi^*}(\Phi^{-2}(\mathbf{x})) \circ \dots \circ f_{\Phi^*}(\Phi^{-n}(\mathbf{x}))(z), \quad (\text{A7})$$

which converges for $n \rightarrow \infty$ towards

$$\lim_{n \rightarrow \infty} F_x^{(n)}(z) = \frac{e_1^u(\mathbf{x})}{e_2^u(\mathbf{x})}, \quad \mathbf{x} \in \mathcal{C}, \quad (\text{A8})$$

for almost all z within any hyperbolic invariant submanifold \mathcal{C} of Φ .

-
- [1] B. J. Bayly and S. Childress, *Geophys. Astrophys. Fluid Dyn.* **44**, 211 (1988).
- [2] E. Ott, Y. Du, K. R. Sreenivasan, A. Juneja, and A. K. Suri, *Phys. Rev. Lett.* **69**, 2654 (1992); Y. Du and E. Ott, *Physica D* **67**, 387 (1993); *J. Fluid Mech.* **257**, 265 (1993).
- [3] J. C. H. Fung and J. C. Vassilicos, *Phys. Fluids A* **3**, 2725 (1991); D. R. Sawyers, M. Sen, and H.-C. Chang, *Chem. Eng. J.* **64**, 129 (1996).
- [4] H. Aref, *Proc. R. Soc. London, Ser. A* **333**, 273 (1990).
- [5] M. M. Alvarez, F. J. Muzzio, S. Cerbelli, A. Adrover, and M. Giona, *Phys. Rev. Lett.* **81**, 3395 (1998); M. M. Alvarez, F. J. Muzzio, S. Cerbelli, and A. Adrover, in *Fractals in Engineering*, edited by J. Levy Vehel, E. Lutton, and C. Tricot (Springer-Verlag, Berlin, 1997), p. 323.
- [6] F. J. Muzzio and J. M. Ottino, *Phys. Rev. Lett.* **63**, 47 (1989); F. J. Muzzio and J. M. Ottino, *Phys. Rev. A* **40**, 7182 (1989).
- [7] I. M. Sokolov and A. Blumen, *Phys. Rev. A* **43**, 6545 (1991); I. M. Sokolov and A. Blumen, *Phys. Rev. Lett.* **66**, 1942 (1991).
- [8] H. Aref, *J. Fluid Mech.* **143**, 1 (1984).
- [9] J. M. Ottino, *The Kinematics of Mixing: Stretching, Chaos and Transport* (Cambridge University Press, Cambridge, 1989).
- [10] J. M. Lopez, A. D. Perry, *J. Fluid Mech.* **234**, 449 (1992).
- [11] V. Rom-Kedar, A. Leonard, and S. Wiggins, *J. Fluid Mech.* **214**, 347 (1990); R. Camassa and S. Wiggins, *Phys. Rev. A* **43**, 774 (1991); A. Pentek, T. Tel, and Z. Toroczkai, *J. Phys. A* **28**, 2191 (1995).
- [12] D. Beigie, A. Leonard, and S. Wiggins, *Chaos Solitons Fractals* **4**, 749 (1994).
- [13] M. Giona, S. Cerbelli, F. J. Muzzio, and A. Adrover, *Physica A* **254**, 251 (1998).
- [14] M. Giona and A. Adrover, *Phys. Rev. Lett.* **81**, 3864 (1998).
- [15] R. Mañé, *Trans. Am. Math. Soc.* **229**, 351 (1977).
- [16] B. V. Chirikov, *Phys. Rep.* **52**, 265 (1979).
- [17] J. M. Greene, *J. Math. Phys.* **20**, 1183 (1979).
- [18] J. Guckenheimer and P. Holmes, *Nonlinear Oscillations, Dynamical Systems and Bifurcations of Vector Fields* (Springer-Verlag, Berlin, 1983).
- [19] V. I. Arnold, *Geometrical Methods in the Theory of Ordinary Differential Equations* (Springer-Verlag, Berlin, 1982).
- [20] D. V. Anosov, *Sov. Math. Dokl.* **4**, 1153 (1963); D. V. Anosov and V. V. Solodov, in *Dynamical Systems IX*, edited by D. V. Anosov, *Encyclopaedia of Mathematical Sciences Vol. 66* (Springer-Verlag, Berlin, 1995).
- [21] S. Cerbelli, M. Giona, A. Adrover, M. M. Alvarez, and F. J. Muzzio, *Chaos, Solitons Fractals* (to be published).
- [22] A. Katok and B. Hasselblatt, *Introduction to the Modern Theory of Dynamical Systems*, Vol. 54 of *Encyclopedia of Mathematics and its Applications* (Cambridge University Press, Cambridge, 1995).
- [23] Ja. B. Pesin, *Math USSR Izvestija* **10**, 1261 (1976); Ja. B. Pesin, *Russ. Math Surv.* **34**, 55 (1977).
- [24] L. M. Barreira, in *Encyclopaedia of Mathematics*, edited by M. Hazewinkel (Kluwer, Dordrecht, 1997), Supplement Vol. I, pp. 405–411.
- [25] G. Gallavotti and E. G. D. Cohen, *Phys. Rev. Lett.* **74**, 2694 (1995); G. Gallavotti and E. G. D. Cohen, *J. Stat. Phys.* **80**, 931 (1995).
- [26] D. Ruelle, *Am. J. Math.* **98**, 619 (1976); D. Ruelle, *Ann. (N.Y.) Acad. Sci.* **356**, 408 (1978).
- [27] G. Gallavotti (unpublished).
- [28] A. Adrover, M. Giona, F. J. Muzzio, S. Cerbelli, and M. M. Alvarez, *Phys. Rev. E* **58**, 447 (1998).
- [29] Y. G. Sinai, *Russ. Math. Surv.* **25**, 21 (1972); D. Ruelle, *Am. J. Math.* **98**, 619 (1976); R. Bowen, *ibid.* **92**, 725 (1970).
- [30] The eventual existence of the eigenvectors $\mathbf{e}_n^u(\mathbf{x})$ means that for $\mathbf{x} \in \mathcal{C}$ there exists an integer n^* , depending on \mathbf{x} , such that, for $n > n^*$, $\Phi^{n^*}(\Phi^{-n}(\mathbf{x}))$ admits eigenvalues greater than 1 in absolute value.
- [31] H. Mori, H. Hata, T. Horita, and T. Kobayashi, *Prog. Theor. Phys. Suppl.* **99**, 1 (1989); Y. Elskens, *Physica D* **100**, 142 (1997).
- [32] A. Manning, *Am. J. Math.* **96**, 422 (1974). In this article, entitled “There are no new Anosov diffeomorphisms of the torus,” Manning shows that any Anosov diffeomorphism of \mathcal{T}^2 is conjugate to a linear hyperbolic one.
- [33] This name, first introduced in Ref. [13], comes from the fact that the trajectories of Eq. (4.1) generate the unstable manifolds of Φ , which are usually indicated in the literature with the letter \mathcal{W} .
- [34] E. M. Ziemniak, C. Jung, and T. Tel, *Physica D* **76**, 123 (1994); G. Karolyi and T. Tel, *Phys. Rep.* **290**, 125 (1997); M. A. F. Sanjuan, J. Kennedy, E. Ott, and J. A. Yorke, *Phys. Rev. Lett.* **78**, 1892 (1997); Z. Neufeld and T. Tel, *Phys. Rev. E* **57**, 2832 (1998).
- [35] The Péclet number $Pe = vL/D$ is the ratio between the characteristic time for diffusion (L^2/D) and advection L/v . If the viscosity is large enough to ensure creeping-flow conditions, diffusion will be slow enough (under most experimental conditions) to be negligible for short and intermediate time intervals. The Thiele modulus is the square root of the characteristic time for diffusion and the characteristic time for reaction. For further details see G. F. Froment and K. B. Bischoff, *Chemical Reactor Analysis and Design* (Wiley, New York, 1979).
- [36] Let μ^* be the invariant ergodic measure for Φ . If Φ and Φ^{-1} are mixing within \mathcal{C} then, for any measurable set Δ , $B \subseteq \mathcal{C}$,

$\lim_{n \rightarrow \infty} \mu^*[\Phi^{-n}(\Delta) \cap B] = \mu^*(\Delta) \mu^*(B)$. Equation (5.22) follows from this property. To prove this, let us consider the characteristic function of the set $B: g_B(\mathbf{x}) = 1$ if $\mathbf{x} \in B$ and 0 otherwise. By definition,

$$\int_{\Delta} g_B(\Phi^{-n}(\mathbf{y})) d\mathbf{y} = \int_{\Phi^{-n}(\Delta)} g_B(\mathbf{y}) d\mathbf{y} = \mathcal{L}[\Phi^{-n}(\Delta) \cap B],$$

where $\mathcal{L}(\cdot)$ is the Lebesgue measure. If Φ is area-preserving and ergodic within \mathcal{C} then $\mu^*(A) = \mathcal{L}(A)/\mathcal{L}(\mathcal{C})$ for any measurable set $A \subseteq \mathcal{C}$. By applying the mixing property

$$\begin{aligned} \lim_{n \rightarrow \infty} \int_{\Phi^{-n}(\Delta)} g_B(\mathbf{y}) d\mathbf{y} &= \mathcal{L}(\mathcal{C}) \mu^*(\Delta) \mu^*(B) \\ &= \mathcal{L}(\Delta) \int_{\mathcal{C}} g_B(\mathbf{y}) d\mu^*(\mathbf{y}), \end{aligned}$$

which is Eq. (5.22) for elementary functions. Since Eq. (5.22) holds for elementary functions, it also holds for continuous functions which can be expressed as the superposition of elementary functions.

- [37] D. Auerbach, P. Cvitanovic, J.-P. Eckmann, G. Gunaratne, and I. Procaccia, Phys. Rev. Lett. **58**, 2387 (1987); G. Gunaratne and I. Procaccia, *ibid.* **59**, 1377 (1987).
- [38] V. I. Arnold and A. Avez, *Ergodic Problems of Classical Mechanics* (Addison-Wesley, Redwood City, CA, 1989).
- [39] D. Auerbach, P. Cvitanovic, J.-P. Eckmann, G. Gunaratne, and I. Procaccia, Phys. Rev. Lett. **58**, 2387 (1987); G. H. Gunaratne and I. Procaccia, *ibid.* **59**, 1377 (1987)
- [40] P. R. Halmos, *Measure Theory* (Van Nostrand, New York, 1950).
- [41] D. F. Escande, Phys. Rep. **3-4**, 165 (1985).